Continuous Solid Particle Flow in Microreactors for Efficient Chemical Conversion

Zong, Jie; Yue, Jun

Link to publication in University of Groningen/UMCG research database

Continuous Solid Particle Flow in Microreactors for Efficient Chemical Conversion

Jie Zong and Jun Yue*

ACCESS | Metrics & More | Article Recommendations

ABSTRACT: The incorporation of flowing nanoparticles or microparticles for use in catalysis as well as in the enhancement of mass transfer in microreactors opens a new avenue for chemical process intensification. In this work, the recent application of handling suspended solid particles in microreactors for carrying out efficient chemical conversions is reviewed, including the use of colloidal suspensions, Pickering emulsions, and catalyst slurries. Emphasis is laid on the effect of the presence of solid particles on the microflow characteristics, mass transfer property, and reaction enhancement, especially in multiphase fluid systems as the most frequently used one in microreactors. A future perspective regarding the potential application of such microreactor systems as well as challenges, especially related to stable flow operation and catalyst recycling, is further provided.
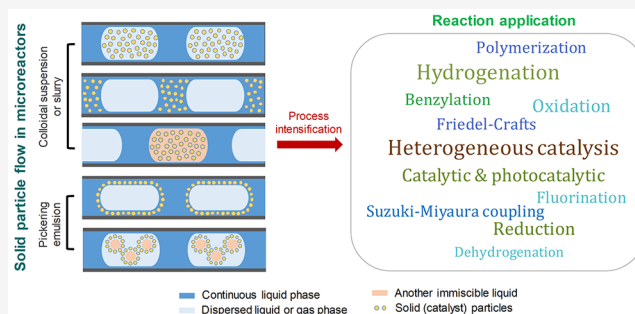
1. INTRODUCTION

Microreactor technology has emerged as an important tool for process intensification via miniaturization, and it has received a large amount of attention in recent decades for new reaction pathway discovery and process development in a continuous flow fashion.[1] Microreactors are characterized geometrically by lateral channel dimensions typically below ca. 1 mm (which can be extended reasonably to a few millimeters provided that the benefits due to miniaturization are maintained).[2] The small reaction channels offer distinct advantages for chemical process improvement, such as substantial heat/mass transfer intensification (primarily due to a significant reduction of the species diffusion path and argumentation of the surface area to volume ratio), and tight process control over the temperature and residence time (distribution).[3,4] These merits allow obtainment of significantly boosted reaction conversions and target product yields in microreactors when compared with conventional batch processing.[5] Due to the small reagent inventory and efficient heat transfer rates, microreactor operations are particularly suitable for reactions with highly hazardous (e.g., flammable, toxic, or explosive) reactants.[3–5] Thus, microreactors have been widely explored as efficient devices for performing a variety of unit operations and chemical transformations.

In multiphase reactions/operations, the application of microreactors has been shown to be well-suited and promising in uncatalyzed or homogeneously catalyzed gas–liquid/liquid–liquid reaction processes, such as absorption,[6] extraction,[7] oxidation reactions,[8,9] and other chemical syntheses,[10,11] as the reaction system only consists of fluid phases that can

flow smoothly in microreactors. In the presence of a solid phase (e.g., as the reactant, catalyst, or product), difficulties may arise in operation with microreactors. Fouling, clogging, and even breakage likely caused by the presence of solid materials could pose a (significant) threat to the lifetime of microreactors.[12] The direct use of solid reactants is rarely applied in microreactors, and it is more convenient to use the liquid form given the fact that many solid reactants can be dissolved in a proper solvent. Better control of the reaction conditions in microreactors allows the synthesis of nanoparticles with smaller size and dispersion than conventional batch synthesis protocols.[13] Strategies such as introducing an immiscible fluid carrier or coupling with ultrasonification have been employed to avoid nanoparticle deposition on the microreactor wall, which are also applicable for other reactions forming solid products in flow.[14–17] Solid catalysts are more attractive than homogeneous ones in terms of catalyst separation and recycle, and are typically used as wall coatings in microreactors (Figure 1a). The thin coating (e.g., 1–10 μm thick) is well suited for fast reactions due to the improved internal diffusion rate.[18] However, tailored coating procedures often need to be developed,[2] and the catalyst removal (e.g., in
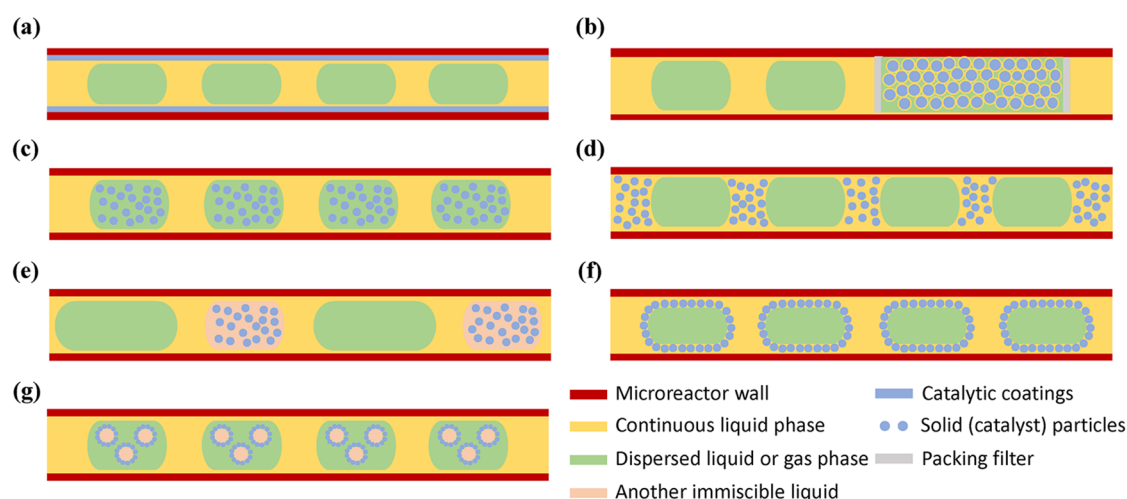
Figure 1. Examples of multiphase reactions in microreactors with wall-coated catalyst (a) or packed bed catalyst (b) and with solid (catalyst) particles suspended in the dispersed (c) or continuous (d) phase or in another dispersed droplet separated by gas bubbles (e), as well as in the possible configuration of flowing Pickering emulsions with the emulsion droplets dispersed in the continuous phase (f) or enclosed in another droplet of the dispersed phase (g). The dispersed phases in parts a, b, and d can be liquids (as droplets) or gases (as bubbles). The flowing solid particles in parts c−e can range in size from nanometer to micrometer, including colloids and slurries.

the case of deactivation) is not trivial without damaging the reactor. An alternative approach is using packed beds in microreactors (Figure 1b), which is more flexible in terms of directly deploying readily available commercial or lab-prepared catalysts as well as catalyst replacement. Such packed bed microreactors exhibit superior heat/mass performance due to the fine particle sizes in use.[2] Nevertheless, this also results in a high pressure drop penalty and complex multiphase hydrodynamics over the bed (e.g., irregular flow patterns, wall channeling, and local dewetting), reducing their application potential to some extent.[19]

Recently, continuous transport of solid catalysts in flow has emerged as another option for performing heterogeneously catalyzed reactions in microreactors,[20] which also allows flexible and multipurpose production.[21] The distribution of solids within the liquid flow can be controlled by adjusting particle−fluid and particle−surface interactions.[12] So far, several solid suspension systems in microflow (Figure 1c−g) have been reported, including colloids (with suspension of nanoparticles), Pickering emulsions (PEs; with solid particles of nanometer or micrometer size stabilized on the two immiscible liquid−liquid interfaces), and slurries (of typically micrometer-sized particles). Colloid nanoparticle catalysts are considered to be semi-heterogeneous combining the advantage of the both high activity of a homogeneous catalyst and the bulk properties (e.g., nanoeffect and high surface area) of a heterogeneous catalyst.[22] Polymer−nanoparticle hybrids, surfactants or ionic liquid-stabilized colloid nanoparticle catalysts have shown potential to catalyze, among others, hydrogenation, oxidation, and C−C coupling reactions.[23] The promising use of colloidal suspensions of noble metal nanoparticle catalysts has been demonstrated in microreactors for enhancing the reaction efficiency, e.g., in the hydrogenation of various alkenes in a gas−liquid−liquid slug flow (Figure 1e).[20] In addition, colloidal suspensions of nanoparticles (e.g., metals, oxides, and carbon nanostructures) were also used as the so-called nanofluids for modifying the functional properties of the base fluid (e.g., water, glycols, alcohols, and oils).[24] Nanofluids have been widely used to enhance the thermal conductivity of the base fluid and thus heat transfer

capabilities, as well as mass transfer (e.g., according to the shuttle mechanism) with or without reactions (e.g., CO_2 absorption and benzylation of toluene) in microreactors.[25,26] The Pickering emulsion (PE) has emerged in the field of biphasic catalysis, which greatly increases the interfacial area available for reactions compared with the classical two-phase emulsion.[27] Developing relevant PE catalysis in flow (Figure 1f and g) is attractive from both a catalytic efficiency and a process engineering point of view.[28] Thus, PE as another type of advanced catalytic system that can be applied in biphasic catalytic reactions has promising application aspects in microreactors for delivering a greener and more sustainable chemical synthesis,[29] as demonstrated in the recent work of Vis et al.[30]

Commercially available or lab-made powder catalysts are usually dispersed on a support for achieving a favorable catalytic activity, the size of which tends to be much larger (e.g., from micrometer to millimeter range). They can be suspended as microparticles in the liquid (e.g., after crushing and sieving to a certain micrometer range) to form a liquid−solid slurry to facilitate their transport and catalysis in microreactors, which allows an easy catalyst separation (by filtration) and extends the versatility of microreactors. Recently, microreactors using such suspension catalysts have been applied under slug flow operation in (photo)catalytic reactions such as (transfer) hydrogenation, fluorination, and polymerization,[31−34] where the catalyst was dispersed in either the continuous or dispersed liquid phase within a biphasic slug flow (Figure 1c−d).

In brief, compared with wall-coated and packed bed microreactors, the incorporation of suspended nanoparticles or microparticles in microreactors opens a new avenue for realizing efficient heterogeneous catalysis and significant process intensification, which is thus the aim of this review. The existing knowledge has been summarized to elucidate the influence of the presence of solid particles (including colloids, PEs, and catalyst slurries) on the microflow characteristics, mass transfer property, and (photo)catalytic reaction enhancement, followed by a discussion of the future challenges and a

perspective for the potential application of such microreactor systems.

2. CONTINUOUS SOLID PARTICLE FLOW FOR CHEMICAL CONVERSIONS IN MICROREACTORS

The application of suspended solid (catalyst) particles in the form of colloids, PEs, and slurries has been reported for a number of reaction cases in microreactors, especially in the presence of multiple fluid phases. This section provides a detailed discussion of the hydrodynamic and mass transfer characteristics during handling such a particle flow in microreactors and their reaction application examples. Some examples in millireactors are also discussed, as these can be easily transferred to microreactor applications for even further process intensification. Thus, a channel (hydraulic) diameter (d_c) of 2 mm has been set as the boundary between microreactors and millireactors to facilitate the discussion.

2.1. Colloidal Nanoparticle Suspension in Microreactors. Colloidal suspensions of nanoparticles are not true solutions but heterogeneous mixtures with a high mobility in flow. Due to the particle size on the nanometer scale, colloidal catalysts present high catalytic activity similar to homogeneous catalysts and possess heterogeneous catalytic properties allowing a relatively easy catalyst separation/recovery.[22,25] They have gained widespread attention in reaction applications[23,35] and slowly progressed into the field of microreactors for achieving significant reaction performance improvement (Table 1, entries 1−12).

2.1.1. Hydrodynamic Characteristics. A good dispersion of colloidal nanoparticles in flow is the prerequisite for their wide application in microreactors. Several classical methods have been used to improve the dispersion of nanoparticles in the prepared suspension, such as adding the dispersant (e.g., sodium dodecyl benzenesulfonate (SDBS),[25] sodium dodecyl sulfate (SDS),[36] and polyvinylprolidone (PVP)[20]), employing magnetic stirring and sonication. The application of dispersants or surfactants is the most economical method to improve the stability of colloids, which can prevent the agglomeration of nanoparticles by reducing the surface tension of the base fluid.[24] For examples, Fe_3O_4-carbon nanotube (CNT)-water with various surfactants (acacia senegal, tetramethylammonium hydroxide, trisodium citrate dehydrate, or sodium laurylsulfonate) can remain stable for 2 weeks.[37] Besides, magnetic stirring is commonly employed in the lab to increase the homogeneity of the prepared colloids by reducing sedimentation of nanoparticles and is mostly applied together with ultrasound.[38] Sonication provides a better dispersion than magnetic stirring.[24] It was also proven that a better dispersion of nanoparticles in the base fluid was achieved by using a probe sonicator rather than a bath sonicator, due to the direct immersion of the probe in the suspension and its higher power delivered to the suspension.[39] The ultrasonication time also affects the colloidal stability.[40−42] There seems to exist an optimum ultrasonication time to reach a good stability (e.g., 60 min reported for the case of the multiwalled CNTs-water nanofluid), with a stability deterioration at prolonged ultrasonication time.[40]

The high mobility of colloidal nanoparticle suspensions in flow makes them behave like a pure liquid flow;[43] thus, they might be treated as a pseudo homogeneous liquid phase with suspension mixture properties.[38] As a result, multiphase flow patterns involving colloidal nanoparticle suspensions appear to be similar to those involving pure liquids; for example, biphasic or triphasic slug flow has been reported for utilizing such suspensions to enhance mass transfer or reaction efficiency in flow.[20,26] In addition, it has been reported that the addition of nanoparticles could alter the wettability of the polytetrafluoroethylene (PTFE) microreactor wall to be more hydrophilic due to nanoparticle deposition,[38] as characterized by the presence of a lubricating film around N_2 bubbles after dispersing nanoparticles in pure water, whereas the film absence was observed during N_2-water slug flow in the PTFE microreactor. The hydrodynamic knowledge largely established in this area can thus be relied on to help rationalize the microreactor design and operation involving colloidal nanoparticle suspensions.[7,44,45]

Slug flow of a gas-colloidal suspension (Figure 1d) has been used to study the promotion effect of SiO_2 nanoparticles (size: 22 nm) on the physical absorption of CO_2 into water in microreactors.[26] The bubble size appeared to decrease when increasing the particle concentration, due to the viscosity increase of the suspension. Such viscosity increase further led to a higher pressure drop (e.g., the range of the pressure drop gradient was from 4.92 kPa/m to 75.58 kPa/m when increasing the particle loading from 1 wt % to 20 wt % at a total flow rate from 80 mL/h to 780 mL/h) through the microreactor (width × height: 0.8 × 0.8 mm),[26] suggesting increased friction between particles and bubbles in the film region and likely more probability of particle collision in the slug, which caused a greater pumping power requirement.[46] The pressure drop under slug flow of N_2-nanofluids (i.e., TiO_2 or Al_2O_3 nanoparticles dispersed in water or its mixture with ethylene glycol) in PTFE microreactors was found to be well described by the model of Kreutzer et al.[47] at the mixture Reynolds number >100, while the model of Warnier et al.[48] provided a better prediction at the mixture Reynolds number <100 due to the consideration of the effect of film thickness and bubble velocity at such low Reynolds numbers.[38] In both model calculations, the nanofluid was simply considered as a pseudo homogeneous liquid phase (e.g., characterized by the mixture viscosity and density).

In gas−liquid−liquid flow hydrogenation operations, the aqueous droplets containing colloidal catalysts were generated and separated by H_2 bubbles, both traveling in the continuous organic slug containing the reaction substrate (Figure 1e and Table 1, entries 1−3).[20,49,50] In this flow pattern, an annular organic film lubricates bubbles and an interfacial organic film separates bubbles and aqueous droplet caps, the presence and thickness of which are crucial in determining the reaction performance. Dewetting and breakage of the annular film were found to easily occur when the channel diameter was relatively large (e.g., 4 mm), showing the importance of using small-diameter microreactors to maintain the surface tension-dominated flow regime instead of the gravity-dominated one. The interfacial film was squeezed out (but did not drain out completely) and redistributed into the annular film at higher flow speeds.[50] Colloidal nanoparticle catalysts in liquids without the presence of gas reactant have also been reported in microreactors for (photo)catalytic reactions in microreactors (Table 1, entries 10−12),[25,51,52] which possibly deal with a (liquid−)liquid−solid flow depending on whether there was a presence of gaseous product or another immiscible liquid or not.

Colloidal nanoparticles can be present either in the dispersed phase (e.g., Figure 1c) or the continuous phase (e.g., Figure 1d and e). The first option provides a more

Table 1. Examples of Reactions Involving Colloidal Nanoparticle Suspensions and Pickering Emulsions in Continuous Flow (Micro)reactors

Entry	Substrate	Catalyst or particles[a]	Product	Reactor[b]	Reaction conditions[c]	Results and advantages of flow operation	Ref
1	Alkenes (1-hexene, cyclohexene, styrene, nitrobenzene and 4-nitrochlorobenzene)	RhNP or PtNP (d_p = 3 nm)	The corresponding alkanes	PTFE capillary microreactor (d_c = 1 mm, L = 2, 10, or 20 m)	Liquid: alkenes in the solvent (cyclohexane, diethyl ether, or 50 vol % diethyl ether and 50 vol % dichloromethane). Colloid: RhPVP or PtPVP in H_2O, 0.5 mM. Gas: H_2; ambient conditions	The conversion was 82% in 0.9 min (for 1-hexene), 30% in 1.2 min (for cyclohexene), 71% in 4.9 min (for styrene), 98% in 0.9 min (for nitrobenzene), and 76% in 0.5 min (for 4-nitrochlorobenzene); catalyst activity ca. 10–100 times higher than that in batch	20
2	Nitrobenzene	PtNP (d_p = 3 nm)	Aniline	Microreactor network (8-fold parallelized; interconnected with polymeric tubes, d_c = 1 mm, L = 30 m)	Liquid: nitrobenzene in diisopropyl ether, 100 mM. Colloid: PtPVP in H_2O, 0.5 mM. Gas: H_2; near ambient conditions	Consistent nitrobenzene conversion (ca. 80%) across each parallel microreactor; continuous online catalyst recycling without significantly changed substrate conversion	49
3	1-Hexene	RhNP (d_p = 3 nm)	1-Hexane	PTFE capillary millireactors (d_c = 3.2 mm and 4 mm, L = 2 m)	Liquid: 1-hexene in decane, 0.8–2.4 M. Colloid: RhPVP in H_2O, 1 mM. Gas: H_2; ambient conditions	100% substrate conversion in ca. 2 min; 150 or 50 times higher production capacity than a single or 8-fold parallel microreactor system (d_c = 1 mm) at comparable conversion and (or shorter) residence time levels	50
4	Nitrobenzene	PdNP (d_p = 3 nm)	Aniline	PTFE capillary microreactor (d_c = 0.86 mm, L = 2 m)	Liquid: nitrobenzene. Colloid: PdTPPTS in glycerol, 10^{-2} M. Gas: H_2; 55 °C, 5 bar.	54% nitrobenzene conversion in 90 s	65
5	Nitrobenzene	PdNP (d_p = 3 nm)	Aniline	Corning millireactor (9×10^{-6} m³ glass plate with millimetric-sized channels)	Liquid: nitrobenzene. Colloid: PdTPPTS in glycerol, 10^{-2} M. Gas: H_2; 55 °C, 4 bar	15% nitrobenzene conversion in 270 s	65
6	Nitrobenzene	PdNP (d_p = 3 nm)	Aniline	IMM R600 stainless steel micromixer, (2.5×10^{-8} m³ in volume)	Liquid: nitrobenzene. Colloid: PdTPPTS in glycerol, 10^{-2} M. Gas: H_2; 55 °C, 3 bar	Below 5% nitrobenzene conversion in 180 s	65
7	Nitrobenzene	PdNP (d_p = 3 nm)	Aniline	PTFE capillary microreactor (d_c = 0.86 mm, L = 2 m)	Liquid: nitrobenzene. Colloid: PdPVP in glycerol, 1 mol %. Gas: H_2; 80 °C, 5 bar	91% nitrobenzene conversion in 210 s; catalyst stable and recyclable after H_2 treatment	65
8	Nitrobenzene	PdNP (d_p = 3 nm)	Aniline	PTFE capillary microreactor (d_c = 0.86 mm, L = 2 m)	Liquid: nitrobenzene. Colloid: PdTPPTS in glycerol, 1 mol %. Gas: H_2; 100 °C, 5 bar	54% nitrobenzene conversion in 150 s	65
9	Nitrobenzene	PdNP (d_p = 3 nm)	Aniline	PTFE capillary microreactor (d_c = 0.86 mm, L = 2 m)	Liquid: nitrobenzene. Colloid: PdQN in glycerol, 1 mol %. Gas: H_2; 80 °C, 5 bar	Below 5% nitrobenzene conversion in 150 s	65
10	Aryl organoborane (e.g., boronic acid) and aryl bromide compounds	Fe/ppm Pd	Biaryl	PFA capillary microreactor (d_c = 0.76 mm, volume of 2–10 mL)	Liquid: aqueous base ($K_3PO_4 \cdot H_2O$, 1.78 M) or neat trimethylamine. Organic carrier: THFA-containing organic reagents (1.15–1.24 equiv of aryl organoborane and 1.0 equiv of aryl bromide compounds). Aqueous nanoparticle stream: 28.5 or 50 mg/mL Fe/ppm Pd suspended in 2 wt % TPGS-750-M in water; 95 °C	Yields of 4-methoxybiphenyl, 1-(4-methoxyphenyl)naphthalene, 2,4,6-trimethylbiphenyl-tert-butyl [1,1'-biphenyl]-4-ylcarbamate, 4-phenyl-3,6-dihydro-2H-pyran, and 3'-chloro-[1,1'-biphenyl]-4-carbaldehyde were 97%, 88%, 93%, 96%, 80%, and 91%, in 10 min, 2 min, 10 min, 8 min, 10 min, and 2 min, respectively, with productivities at 517, 2934, 528, 720, 360, and 2853 mg/h	52
11	Toluene and benzyl chloride	$FeCl_3$–SiO_2 (d_p = 70 nm)	Monobenzyl toluene and dibenzyl toluene	PFA capillary microreactor (d_c = 1 mm)	Liquid: toluene. Nanofluid: 5–15 wt % $FeCl_3$–SiO_2 in benzyl chloride with SDBS, 0.01–0.04 mass ratio; 100 °C	78.7% benzyl chloride conversion and total selectivity of 94.2% (to monobenzyl toluene and dibenzyl toluene) in 30 min over 10 wt % $FeCl_3$-SiO_2; catalyst recycled and reused for three times	25
12	Nitrobenzene	TiO_2 (d_p = 5–10 nm)	Aniline	PFA capillary microreactor (d_c = 1 mm)	Liquid: nitrobenzene (3.3 mg/mL) and formic acid dissolved in isopropanol. Nanofluid: TiO_2 and polyethylene glycol-400 in H_2O, 0–1.2 mass ratio of TiO_2 to nitrobenzene; 20 °C	88.7% nitrobenzene conversion and 64% yield of aniline under a mass ratio of 0.4 and in 10 min; high photocatalytic activity of TiO_2 catalyst retained after four cycles	51
13	Benzaldehyde dimethyl acetal	SiO_2-stabilized Pickering emulsion	Benzaldehyde	Tube-in-tube microreactor (with a 100 μm inner diameter fused silica tubing and a 0.8 mm inner diameter FEP tubing in a coaxial flow geometry)	Dispersed phase: water (containing 0.1 M HCl). Continuous phase: 4-propylguaiacol (containing 1 M benzaldehyde dimethyl acetal and 2 wt % silica); ca. 20–90 °C	Benzaldehyde yield increased from 10% in the FBS (flow biphasic system) to 90% in the FPE (flow Pickering emulsion) after 22 min at room temperature; 100% conversion in 2 min in the FEP at 60 °C vs ca. 18 min in the FBS	30

Table 1. continued

Entry	Substrate	Catalyst or particles[a]	Product	Reactor[b]	Reaction conditions[c]	Results and advantages of flow operation	Ref
14	Benzaldehyde dimethyl acetal	SiO$_2$-stabilized Pickering emulsion	Benzylidene malononitrile	Tube-in-tube microreactor (details in entry 13)	Dispersed phase: water (containing 0.032 M HCl). Continuous phase: 4-propylguaiacol (containing 0.16 M benzaldehyde dimethyl acetal, 0.4 M malononitrile, 0.016 M 2-(1-ethylpropyl)piperidine, and 2 wt % silica); 90 °C	100% benzaldehyde dimethyl acetal conversion in the FPE, with 69% intermediate product (benzaldehyde) yield and 25% final product (benzylidene malononitrile) yield in 34 min; 34% substrate conversion in the FBS with 10% intermediate and 17% final product yields under identical conditions	30

[a]d_p (mean) particle size; RhNP, rhodium nanoparticle; PtNP, platinum nanoparticle; PdNP, palladium nanoparticle. [b]d_o inner (hydraulic) diameter of the (micro)reactor; L, reactor length; PTFE, polytetrafluoroethylene; PFA, polyfluoroalkoxy; FEP, fluorinated ethylene propylene. [c]THFA, tetrahydrofolic acid; SDBS, sodium dodecyl benzenesulfonate.

narrowed residence time distribution and is inherently safe from the fouling or clogging caused by the deposition of nanoparticles on the microchannel wall.[53] Besides, a modification of the microreactor surface (e.g., to be superhydrophobic) can decrease the possibilities of aggregation and sedimentation of nanoparticles in microreactors, due to the reduced wall shear stress in the slip flow regime.[43]

Moreover, when it concerns colloidal suspensions of magnetic nanoparticles (i.e., ferrofluids), a unique approach is provided for manipulating the flow of such ferrofluids in microreactors by applying external magnetic fields in addition to the action of pressure-driven flow.[54] For example, the breakup, deformation, and lateral migration of ferrofluid droplets in a shear flow can be modulated by the applied (uniform) magnetic field,[54−56] which has attracted much attention in microfluidics. The use of ferrofluids also opens new possibilities for the intensification of mass transfer in microreactors, e.g., in the presence of inert magnetic particles suspended and transported in flow (*vide infra*).

2.1.2. Mass Transfer. The addition of nanoparticles to promote gas−liquid mass transfer has been shown in conventional reactors such as bubble columns, for which several arguable mechanisms of mass transfer enhancement have been proposed.[57−59] For example, nanoparticles can enhance mass transfer by repeating the cycle of gas absorption and desorption between the boundary layer and the bulk liquid (shuttle mechanism), adhering on the bubble surface to strengthen its stiffness and reduce the coalescence (bubble breaking effect), or changing the hydrodynamics of the surrounding fluid (boundary layer mixing mechanism).

Recently, the enhancement of gas−liquid mass transfer by SiO$_2$/H$_2$O nanofluid (22 nm particle size) was investigated in a microchannel under the slug flow regime (Figure 1d) for CO$_2$ absorption.[26] The mass transfer enhancement factor was found to be ca. 2.5 times higher with 20 wt % silica concentration than that with 1 wt % silica concentration at a high gas−liquid flow ratio. The enhancement was obvious especially at relatively high silica loadings and gas−liquid flow ratios, which is ascribed to the facts that more particles could be transferred from the slug to the film region and the liquid was not saturated, giving intensification potential via the additional particle adsorption and transport (i.e., according to the shuttle mechanism). The addition of nanoparticles (SiO$_2$ and BaSO$_4$) on improving the liquid-phase mixing in microreactors was also shown in the work of Dong et al.[60] and explained by the enhancement from Brownian movement of nanoparticles, despite the adverse effect of the liquid viscosity increase that might weaken the mixing performance.

The liquid−solid (external or internal) mass transfer coefficient is often required to be known for predicting and interpreting the microreactor performance when using colloidal nanoparticle catalysts. A rough (order of magnitude) estimation can be made based on the classical approach, e.g., using the two-film mass transfer theory[20] or the concept of effective factors.[25] However, a more precise estimation should further consider phenomena related to the motion of nanoparticles in the solution such as the additional diffusion resistance caused by the often used capping agent (to stabilize nanoparticles) and other local hydrodynamic effects (if present), an area still to be further explored.

In addition, external magnetic or ultrasonic fields can be used to enhance biphasic (gas−liquid, liquid−liquid) mass transfer in the presence of flowing nanoparticles in micro-
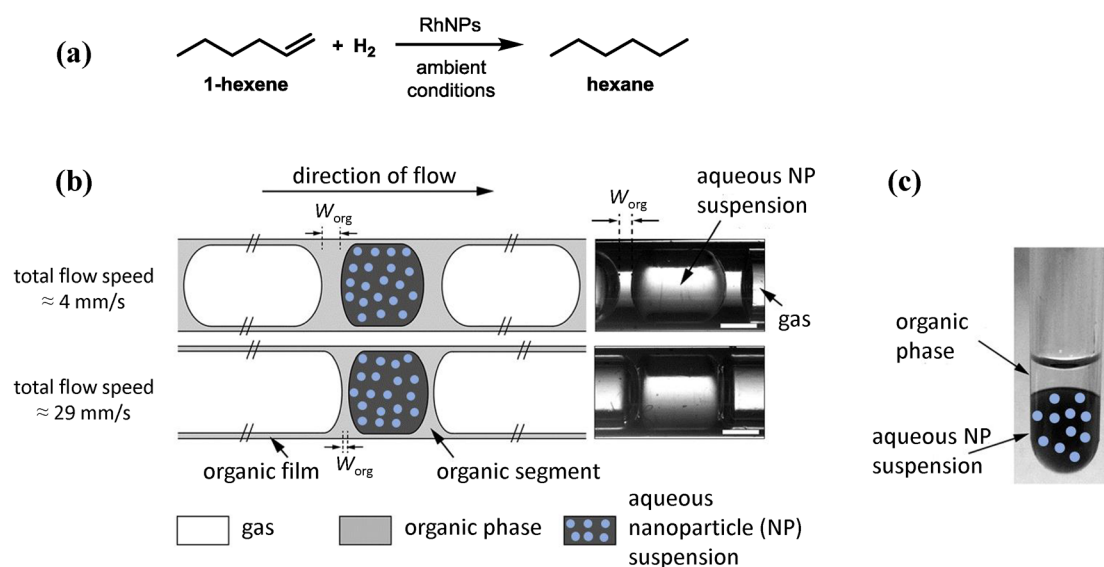
Figure 2. Gas−liquid−liquid hydrogenation of alkenes to the corresponding alkanes in microreactors using colloidal catalysts. (a) Reaction scheme of 1-hexene hydrogenation; (b) schematics of triphasic slug flow; and (c) catalyst recovery from the aqueous−organic phase separation. Adapted with permission from ref 20. Copyright 2014 Royal Society of Chemistry.

reactors. An up to 70% improvement in the overall mass transfer coefficient was found for the extraction of succinic acid from *n*-butanol to water, by adding magnetic nanoparticles (MNPs) of Fe_3O_4 in the organic phase (at an optimum concentration of 0.005 wt %) excited remotely with a static magnetic field.[61] This enhancement is due to the actuation of MNPs that induced additional (chaotic) advection between immiscible fluid streams. Fe_3O_4-derived nanobars were placed inside droplets generated in the microchannel, which created many vortexes (by using a common magnetic stirrer) to effectively stir the fluid flow as well as microparticles in the droplet.[62] A rapid mixing was thus achieved, without destabilizing and rupturing droplets. A measurable improvement of the gas−liquid mass transfer was reported under a slug flow of oxygen and dilute suspensions of Fe_3O_4 MNPs in water through microreactors, as a result of the improved mixing in the film region surrounding bubbles by spinning MNPs under transverse rotating magnetic fields.[63] The combination of ultrasound and Fe_3O_4 nanoparticles was also reported to significantly enhance the liquid−liquid two-phase mass transfer rates in Cu(II) removal from aqueous solution using D2EHPA solvent in a microreactor.[64] Besides the stimulation of liquid phases, the ultrasonic wave further induced nanoparticle movements from the organic to the aqueous phase. This has caused the presence of a very fine droplet distribution at low flow rates or a chaotic mixing pattern at high flow rates to promote mass transfer, in comparison to slug or parallel flow in a plain microreactor (without sonication and nanoparticles).

2.1.3. Reaction Application Examples. Table 1 depicts typical reaction examples of using colloidal catalyst particles in microreactors.

Khan's group studied the transitional metal-catalyzed hydrogenation of various alkenes (e.g., 1-hexene, cyclohexene, styrene, nitrobenzene, and 4-nitrochlorobenzene) to the corresponding alkanes, a reaction type of relevance to the pharmaceutical industry, in a PTFE microreactor (Table 1, entry 1).[20] The reaction was operated under a gas−liquid−liquid slug flow (Figure 1e), where aqueous droplets were loaded with rhodium nanoparticle (RhNP) or platinum

nanoparticle (PtNP) catalyst stabilized by PVP, in the presence of gas (hydrogen) bubbles and a continuous organic slug (containing alkenes). At a constant flow rate of the aqueous and organic phases, increasing the gas flow rate caused longer bubble lengths. Despite the shortened residence time, the mass transfer of hydrogen and the alkene substrate was thought to be accelerated, because of the reduced distance (i.e., the slug length, w_{org}, see Figure 2) to reach the catalyst near the aqueous−organic interface. As a result, the 1-hexene conversion over the colloidal RhNP catalyst reached 82% in 0.9 min in the microreactor under ambient conditions, while it required 30 min to reach similar conversions in a batch reactor. The much enhanced mass transfer in the microreactor further afforded a significantly higher conversion of other alkenes, as mentioned above over the colloidal RhNP or PtNP catalyst at a reaction time of about 10−100 times smaller than that in batch under identical conditions. The colloidal PtNP catalyst in microflow was also estimated to provide higher activities in the hydrogenation of nitrobenzene than the wall-coated PtNP catalyst in microreactors. Moreover, a simple phase separation by decantation allowed the facile recovery and reuse of the colloidal catalyst in the aqueous phase (Figure 2c), and the consistently high activity of the colloidal PtNP catalyst has been demonstrated in the hydrogenation of nitrobenzene in six catalyst recycles.[20] The reaction productivity increase could be further achieved via utilizing either parallelized microreactor networks integrated with online catalyst recycle (Table 1, entry 2)[49] or larger channel dimensions in which the desired flow pattern for rapid mass transfer as depicted in Figure 2b could still be maintained (Table 1, entry 3).[50]

Another example applying colloidal palladium nanoparticle (PdNP) catalyst dispersed in glycerol for hydrogenation reactions was demonstrated by Reina et al.[65] under three continuous flow systems (i.e., IMM R600 micromixer, Corning millireactor, and tube-in-tube PTFE microreactor). The performance of these reactors was compared on the hydrogenation of nitrobenzene to aniline (a versatile starting material for synthesizing fine chemicals) catalyzed by the prepared colloidal PdNP catalyst stabilized by trisodium 3-

bis(3-sulfonatophenyl)phosphanylbenzenesulfonate (TPPTS) (Table 1, entries 4−9). The tube-in-tube microreactor proved to be the most suitable system, achieving 54% conversion within 90 s at 55 °C. In contrast, the micromixer showed less than 5% conversion within 180 s, while the Corning millireactor required 270 s to achieve 15% conversion. It was revealed that the tube-in-tube microreactor, with a gas porous Teflon membrane inserted into a PTFE tube, could hold a maximum pressure of 12 bar H_2 and allowed for a balanced gas−liquid mass transfer facilitating the optimal effusion of hydrogen into the two immiscible phases (i.e., nitrobenzene and the glycerol suspension of the colloidal catalyst). A triphasic bubbly or slug flow regime was formed in this microreactor (however, no further flow details were mentioned), leading to a better solubilization of molecular hydrogen. The much lower conversion in the other two reactors was ascribed to a poor control over the flow pattern and thus mass transfer of H_2 therein. An annular flow regime was observed in the micromixer even with low hydrogen pressures (1−3 bar H_2), where the glycerol layer wetted the stainless steel reactor wall with H_2 and nitrobenzene being blown out without creating the desired gas−liquid−liquid slug flow as illustrated in Figure 2b. In the Corning glass microreactor, although the gas−liquid mass transfer was significantly better than that in the micromixer, the triphasic slug flow was also not achieved. Instead, large H_2 bubbles and small droplets of nitrobenzene were observed due to the high viscosity of the glycerol suspension.

They further investigated the hydrogenation of nitrobenzene in this tube-in-tube microreactor with colloidal PdNP catalysts stabilized by quinidine (QN) or PVP.[65] A high 91% conversion over the catalyst stabilized by PVP was found within 210 s at 80 °C, accompanied by a 100% selectivity to aniline. This is in strong contrast to the 7200 s needed in batch reactors for a similar level of conversion. However, the respective conversions for the colloidal catalysts stabilized by QN and TPPTS are <5% (in 150 s at 80 °C) and 54% (in 150 s at 100 °C) in the microreactor. The low activity of these two catalysts could be due to their poor stability in flow (e.g., induced by the mechanic stress from pumps), causing nanoparticle aggregation. The colloidal catalyst stabilized by PVP proved to be robust in flow and could be recycled via the product extraction of the glycerol solution (with toluene). However, a significant activity drop of the recycled catalyst was observed in the microreactor, possibly due to the oxidation of metal nanoparticles and/or the particle surface interaction with certain chemicals incurred during the workup. A possible method to recover the catalyst activity is via further regeneration under hydrogen atmosphere, which was successfully demonstrated in batch reactors and can be potentially operated in flow as well.

Recently, metal (Fe/ppm Pd nanoparticle)-catalyzed Suzuki−Miyaura coupling reactions in perfluoroalkoxy alkane (PFA) microreactors were reported (Table 1, entry 10).[52] Separate streams of the organic phase (tetrahydrofurfuryl alcohol (THFA) as the carrier containing the organic reagents), Fe/ppm Pd nanoparticles suspended in an aqueous micellar medium (containing the surfactant TPGS-750-M), and an aqueous base ($K_3PO_4 \cdot H_2O$) were mixed prior to the synthesis in the microreactor under 95 °C. A 97% yield of 4-methoxybiphenyl, 88% yield of 1-(4-methoxyphenyl)-naphthalene, and 93% yield of 2,4,6-trimethylbipheny were obtained within 10 min, 2 min, and 10 min, respectively. However, to synthesize products with high melting points or

crystallinity (e.g., *tert*-butyl-[1,1′-biphenyl]-4-ylcarbamate), neat triethylamine (TEA) was used as the organic base instead, as a considerable amount of the precipitated gelatinous TPGS-750-M would appear from water after the addition of phosphate base for a long reaction time, which could clog the microreactor. Accordingly, a 96% yield of *tert*-butyl-[1,1′-biphenyl]-4-ylcarbamate, 80% yield of 4-phenyl-3,6-dihydro-2H-pyran, and 91% yield of 3′-chloro-[1,1′-biphenyl]-4-carbaldehyde were realized using neat TEA within 8 min, 10 min, and 2 min, respectively.

Besides colloidal nanoparticles of noble metals, nanofluids featuring the use of colloidal suspensions of metal oxides as the catalyst (support) were also reported in microreactors.[25,51] Benzylation of toluene with benzyl chloride generating monobenzyltoluene and dibenzyltoluene (both as the main components of heat transfer fluids) was conducted in a PFA capillary microreactor.[25] The catalyst-containing nanofluid was prepared by suspending silica-supported $FeCl_3$ catalysts in benzyl chloride with the addition of SDBS to reduce the catalyst particle size (to around 70 nm) and improve the nanofluid stability. A moderate mass ratio of catalyst to benzyl chloride (0.02) was chosen to increase the reaction efficiency and avoid clogging of the microreactor (observed at higher catalyst loadings due to the accelerated agglomeration of nanoparticles in the nanofluid). The benzyl chloride conversion in the microreactor could reach 78.7% in 30 min at 100 °C over the 10 wt % $FeCl_3$ impregnated on silica with a total selectivity of 94.2% to monobenzyltoluene and dibenzyltoluene, and approached 100% in 60 min (Table 1, entry 11). The flow pattern in the microreactor was not mentioned in the research, which could be complex given the possible presence of gaseous product (HCl). Furthermore, the catalyst was recycled by filtration followed by calcination and then reused (in the form of nanofluid) in the microreactor three times. A gradual activity loss was noticed, likely associated with the particle aggregation and oxidation of catalysts in the recovering procedure.

Later, the same group applied TiO_2/H_2O nanofluid as the photocatalyst for the reduction of nitrobenzene to aniline under UV irradiation in capillary microreactors.[51] The nanofluid was prepared by mixing TiO_2 ($d_p = 5{-}10$ nm) and polyethylene glycol-400 in water, and the reactant solution contained nitrobenzene and formic acid dissolved in isopropanol. Upon mixing these two fluids in the photocatalytic microreactor (with no details provided for the operating flow pattern), the nitrobenzene conversion and aniline yield both exhibited a volcano-type shape with respect to the catalyst loading, which reached the highest value (being ca. 88% and 64%, respectively) at a TiO_2/nitrobenzene mass ratio of 0.4 (Table 1, entry 12). The dropped activity at higher TiO_2 loadings was considered to be caused by serious particle agglomeration. This continuous flow synthesis protocol achieved a remarkably higher photonic efficiency (0.0142) than that in batch (0.0086). The catalyst could be recovered by centrifugation, and subsequent washing (with isopropanol) and drying at room temperature. However, the reusability test in the microreactor under several cycles revealed a gradual loss of catalyst activity, possibly caused by the catalyst loss in the workup.

2.2. Pickering Emulsion in Microreactors. PE is an emulsion stabilized by solid particles that adsorb on the two immiscible liquid−liquid (e.g., water−oil) interfaces. The size of the solid particles ranges from about 10 nm to 100 μm, and
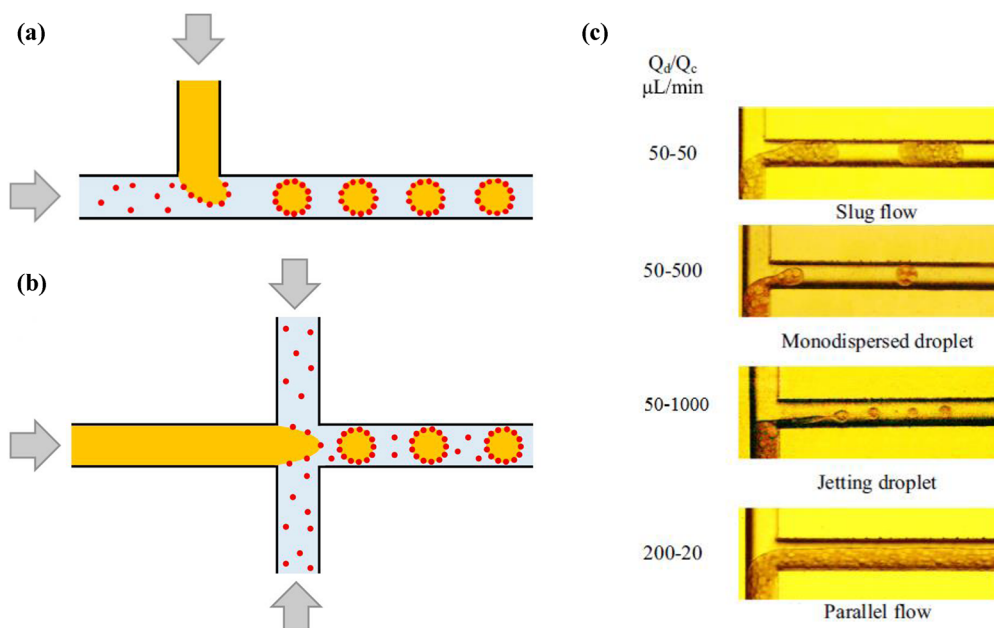
Figure 3. Examples of microfluidic devices with a T-junction (a) or flow-focusing inlet mixer (b) for Pickering emulsion preparation, and the flow patterns observed in a T-junction microchannel for the Pickering emulsion (water in ethyl acetate stabilized by SiO$_2$)−water system as a function of the flow ratio between the dispersed and continuous phases (Q_d/Q_c) (c). Parts a and b were reproduced from ref 66. Copyright 2019 Elsevier. Part c was reproduced from ref 68. Copyright 2021 Elsevier.

that of PE droplets is usually from 10 to 1000 μm.[28] PE has received much attention for its applications in the food, pharmaceutical, and biomedical industries and, more recently, in catalysis, and it has proven to be a versatile tool especially for biphasic catalysis.[27] Thus, it offers promising aspects for boosting the reaction efficiency in multiphase microreactors.[30]

2.2.1. Hydrodynamic Characteristics. Recently, microfluidic emulsification has been used to prepare PEs.[66] A typical microfluidic device for such a process consists of a T-junction (Figure 3a) or flow-focusing inlet mixer (Figure 3b), where a droplet of the dispersed phase is formed at the mixer junction in another continuous fluid carrier. The flow conditions should be tuned such that the droplet formation time is long enough for its surface to be covered by solid particles and to avoid coalescence between droplets. Microfluidic emulsification presents some advantages over other methods (e.g., the rotor-stator homogenization, high-pressure homogenization, and (ultra)sonication), including a superior control of the droplet size, no extensive mechanical shear (causing otherwise the particle disruption or aggregation), and no heat production (with no risks of particle/emulsion destabilization).[66] This microfluidic approach allows coupling the efficient synthesis of PEs and their reaction enhancement in the same microreactor, e.g., biphasic reactions under the liquid−liquid slug flow (Figure 1f) or monodispersed droplet flow regime.[30]

Alternatively, PEs can be prepared via conventional procedures and then fed to the microreactor for a continuous flow reaction, without generating a significant pressure drop in a similar manner as for solid particles in a packed bed reactor.[67] The liquid−liquid flow behavior of the Pickering emulsion−water system was studied in one microchannel.[68] PEs were obtained by dispersing water in oil (ethyl acetate) stabilized by SiO$_2$ particles (modified to be hydrophobic), using ultrasonication followed by vigorous mixing in batch. Four stable flow patterns, namely slug flow, monodispersed droplet flow, jetting droplet flow, and parallel flow, were

observed (Figure 3c). The former two flow patterns could be attractive for potential reaction applications given their well-defined interfacial area and good mixing properties, implying that the reactions are confined in the droplets where PEs are dispersed (see Figure 1g as well). The encapsulation of modified SiO$_2$ particles in PEs allowed a stable microreactor operation without channel fouling or blockage. In comparison, during the immiscible flow of water and particle-laden ethyl acetate in the microchannel, SiO$_2$ particles were found to be easy to deposit at the bottom due to gravity and to adhere to the microchannel wall.

The unique interface self-assembly property of solid particles in PEs reduces the possibility of collision and coalescence between the adjacent emulsion droplets.[28] This helps achieve a stable emulsion flow and finely controlled liquid−liquid interface in the microreactor.[30,68] In addition, this decreases the possibility of particles clumping together or adhering to the inner walls, suppressing the fouling or blockage of microreactors.

2.2.2. Mass Transfer. PE offers attractive mass transfer properties beneficial to biphasic catalytic reactions. Due to the uniform dispersion of micrometer-sized droplets compartmentalized by a layer of (inert) particles in another immiscible liquid, a well-defined and high interfacial area and a short diffusion path of species inside the droplet could be achieved in conventional reactors as well as microreactors.[69] The reagents and homogeneous catalysts can reside in (each of) the two phases. Another attractive option is to catalyze reactions using solid catalyst particles at the interface.[70] The adsorption of solid particles is often considered irreversible at the liquid−liquid interface due to a very high desorption energy (which can be several orders of magnitude higher than the thermal motion energy of molecules).[71] The stabilizing effect of particles (i.e., preventing coalescence) on emulsions implies an improved interfacial area for mass transfer when compared with that without particle addition. The interfacial area is
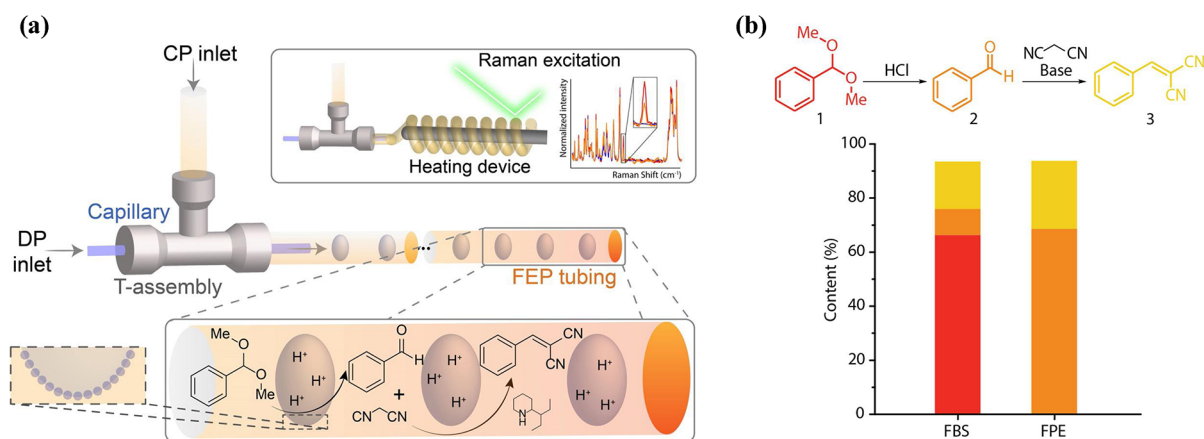
Figure 4. (a) FPE catalysis in a tube-in-tube microreactor with 4-propylguaiacol as the continuous phase (CP) and water as the dispersed phase (DP). Top inset: in situ Raman spectroscopy monitoring of the acid-catalyzed deacetalization reaction of benzaldehyde dimethyl acetal. Bottom inset: acid−base-catalyzed deacetalization−Knoevenagel reaction scheme in the FPE. (b) Product distribution for the deacetalization−Knoevenagel condensation in the microreactor for the FBS and FPE. Red bars are for benzaldehyde dimethyl acetal (1), orange bars for benzaldehyde (2), and yellow bars for benzylidene malononitrile (3). Reaction conditions: 0.16 M benzaldehyde dimethyl acetal, 0.4 M malononitrile, and 0.016 M 2-(1-ethylpropyl)piperidine in 4-propylguaiacol, 0.032 M HCl in water, 2 wt % silica (if present) in the organic phase, 20 μL/min total flow rate, 90 °C. Reproduced with permission from ref 30. Copyright 2020 Wiley.

related to the amount of stabilizing particles which could control the size of droplets. It was shown that a larger particle loading allowed the formation of smaller droplets of PE and then increase of the interfacial area.[72] Nevertheless, the "plateau" of droplet size was observed with the possible presence of excess solid particles in the continuous phase,[73] which led to an increased viscosity of PE and the cluster of solid particles. The occupancy of particles at the interface also tends to diminish the effective mass transfer area. During the saponification reaction between sodium hydroxide (in the continuous aqueous phase) and benzoyl chloride (in the dispersed organic phase) in a stirred tank, a steady decrease of the molar mass transfer flux up to 26% was found when increasing the loading of silica nanoparticles from 0.5 wt % to 1.5 wt %. This flux decrease is due to the higher coverage (about 23% at 1.5 wt % loading) of the droplet interface with nanoparticles. Thus, in order to maximize the effective mass transfer rate for an efficient conversion in PEs, these opposite effects need to be carefully addressed, e.g., by selecting the appropriate particle type, shape, loading, and reactor operating conditions in order to keep the interfacial area largely accessible for mass transfer.[74]

To the best of our knowledge, there are no detailed studies that investigate the interfacial mass transfer of substrates and products in microreactors with continuous flow of PEs. Only one recent piece of literature reported reaction applications in such microreactors.[30] Biphasic catalysis in PEs in microflow was shown to enhance the (tandem) reaction efficiency, owing to the presence of inert solid particles at the interface that increased the interfacial area available for reaction and reduced the mutual contact of homogeneous acid/base catalysts present in different liquid phases (Table 1, entries 13 and 14). More details are found in section 2.2.3.

2.2.3. Reaction Application Examples. The use of PEs for reaction efficiency increase has been demonstrated to some extent in batch and flow reactors, primarily thanks to their enhanced mass transfer and well-controlled interface catalysis. Some recent examples include the coupling of the KHSO4-catalyzed glycerol dehydration reaction with in situ product (acrolein) extraction to the organic phase in batch,[75] the

addition reaction of various alcohols with 3,4-dihydro-2H-pyran (both in the following toluene phase) catalyzed by H_2SO_4 distributed in the aqueous droplet of a PE packed into a column reactor,[69] and the use of Pd-based solid catalysts to stabilize and catalyze the reduction of nitrobenzene with $NaBH_4$ in a water/toluene PE in batch.[70]

Only one literature work reported applications of continuous flow Pickering emulsion (FPE) catalysis in microreactors,[30] using the acid-catalyzed deacetalization of benzaldehyde dimethyl acetal to benzaldehyde as a model reaction (Table 1, entry 13). The PE droplet was obtained using a tube-in-tube microreactor fed with an acidic aqueous phase and an organic solvent (4-propylguaiacol containing the reactant and dispersed silica particles) (Figure 4a). Compared with the simple flow biphasic system (FBS) in the same microreactor (i.e., without silica addition), the FPE significantly boosted the reaction efficiency. The product yield was increased from 10% in the FBS to 90% in the FPE after a reaction time of 22 min at room temperature. A full conversion was achieved in only 2 min in the FPE at 60 °C, in contrast to ca. 18 min in the FBS. This reactivity enhancement was ascribed to the higher aqueous−organic interfacial area in the FPE due to a better stability of droplets stabilized by silica (thus preventing droplet coalescence as observed in the FBS). The benefits of the FPE in the tandem catalysis were further demonstrated in the same microreactor system via the deacetalization−Knoevenagel condensation (by further adding a base catalyst and malononitrile as the second substrate in the oil) (Table 1, entry 14). It enabled a full conversion of benzaldehyde dimethyl acetal at 90 °C in 34 min, with the intermediate product (benzaldehyde) yield at 69% and final product (benzylidene malononitrile) yield at 25%. Under identical conditions, the respective intermediate and final product yields are 10% and 17% at only 34% benzaldehyde dimethyl acetal conversion in the FBS (Figure 4b). This implies that solid particles in the FPE acted as a physical barrier at the liquid−liquid interface and thus limited the mutual destruction of the acid and base catalysts, whereas a much faster acid−base quenching was present in the FBS, leading to a much inferior tandem reaction performance.

Table 2. Examples of Reactions Involving Slurry Catalysts in Continuous Flow (Micro)reactors

Entry	Substrate	Catalyst[a]	Product	Reactor[b]	Reaction conditions[c]	Results and advantages of flow operation	Ref
1	3-Methyl-1-pentyn-3-ol	5 wt % Pd/SiO$_2$ (d_p = 40 μm)	3-Methyl-1-penten-3-ol	PFA capillary microreactor (d_c = 1.65 mm, L = 8.8 and 14.4 m)	Slurry: 0.11 M 3-methyl-1-pentyn-3-ol in ethanol, 0.22 M quinoline (modifier), n-pentanol (internal standard) and Pd/SiO$_2$ (3.5 g/L). Gas: H$_2$; 20 °C, 1.3 bar	∼90% 3-methyl-1-pentyn-3-ol conversion in 150 s, with close to 100% 3-methyl-1-penten-3-ol selectivity; kinetic operation in this gas–liquid–solid slug flow contact mode	31
2	Ethyl cinnamate	Pd/C	Ethyl 3-phenylpropanoate	Corning advanced-flow microreactors (d_c ≈ 1 mm)	Liquid: 0.35 or 0.55 M ethyl cinnamate in ethyl acetate. Slurry: Pd/C in ethanol (0.25 or 0.5 wt %). Gas: H$_2$; 25–75 °C, 5–12 bar	98% yield of ethyl 3-phenylpropanoate at 75 °C in 18 s using 0.5 wt % catalyst slurry, giving 51.3 g/h productivity; only 48% yield with 27.8 g/h productivity at 25 °C under the same conditions	91
3	Resorcinol	5 wt % Rh/γ-Al$_2$O$_3$ (d_{50} ≈ 45 μm)	1,3-Cyclohexanedione	Capillary millireactor (d_c = 3.86 mm, L = 5 m)	Slurry: resorcinol (8–30.5 wt %) and NaOH (12.6 wt %) dissolved in water and mixed with 5% Rh/Al$_2$O$_3$ (typically 1 g in 75 mL solution of resorcinol). Gas: H$_2$; 50–100 °C, 3–17 bar	7 times higher reaction rate at 70–100 °C than that in batch autoclave under equivalent reaction conditions	92
4	Isophorone	5 wt % Pd/C or Rh/C, (d_{10} = 2.68 μm, d_{50} = 18.28 μm)	Trimethyl cyclohexanone	Capillary millireactor (d_c = 3.86 mm, L = 5 m)	Slurry: 40–100 mL isophorone with 1 g of humid Pd/C or Rh/C. Gas: H$_2$; 60–100 °C, 6–12 bar	The reaction rate increased by ∼5–8 times compared with the batch autoclave system; reaction under kinetic control	21
5	Resorcinol	5 wt % Pd/C	1,3-Cyclohexanedione	Heat exchange reactors with rectangular microchannels (1–2 mm in width; forming a zigzag shape; 3 mL of the total process volume)	Slurry: resorcinol (24 wt %) and NaOH (12.6 wt %) dissolved in water and mixed with 5% Pd/C (0.15 g in 75 mL solution of resorcinol). Gas: H$_2$; 85 °C, 6–7 bar	Decreased reaction rate with the reduced channel cross-section, due to the quicker and more significant channel blockage; bigger channels better suited for the reaction with slurry catalyst	93
6	Glycerol	1 wt % Au/C	Oxidation products (e.g., glyceric acid and dihydroxyacetone)	Cordierite monolith (62 channels per cm^2) housed in a stainless steel tubing, operated as the structured down flow slurry bubble column reactor (SBCR)	Slurry: 0.6 M glycerol and 0.6 M NaOH in water, 1 wt % Au/C (glycerol/metal molar ratio from 1165 to 4730). Gas: air; 60 °C, 2.5–14 bar	Two orders of magnitude higher reaction rate than that in autoclave studies; ca. equal quantities of glyceric acid and dihydroxyacetone produced in this SBCR vs a highly selective formation of glyceric acid in the autoclave and coated monolith reactor, inferring the faster oxygen transport in the SBCR	94
7	Phenoxyacetic acid	CMB-C$_3$N$_4$	Fluoromethoxybenzene	FEP capillary microreactor (d_c = 1.6 mm, volume of 17 mL)	Liquid: the solvent (acetonitrile–water mixture), with the reaction mixture (0.7 mmol phenoxyacetic acid and 2.1 mmol Selectfluor mixed in acetonitrile and water; both 1.75 mL) introduced via a sample loop. Slurry: CMB-C$_3$N$_4$ (17 mg/mL) suspended in ([Bmim]BF$_4$)–water mixture. Gas: N$_2$. Light: 420 nm LED	94% fluoromethoxybenzene yield in 14 min; a three-step filtration–extraction could separate the product and recover the catalyst from [Bmim]BF$_4$	33
8	Methyl methacrylate (MMA)	mpg-C$_3$N$_4$ (d_p ≈5 μm)	Polymethyl methacrylate (PMMA)	PFA capillary microreactor (d_c = 1.6 mm, L = 3.8–25 m)	Slurry: mpg-C$_3$N$_4$ (0–3 mg/mL) in the reaction mixture (1–5 M methyl methacrylate in dimethyl sulfoxide, with 4-cyano-4-(dodecylsulfanylthiocarbonyl)-sulfanylpentanoic acid as the RAFT agent and triethanolamine as the reducing agents). Gas: N$_2$. Light: 360–370 nm LED	The MMA conversion increased from 19% to 46% in 100 min when the catalyst loading changed from 0 to 0.5 mg/mL and slightly decreased when further increasing the loading to 3 mg/mL; the measured apparent rate constant almost doubled that of batch reactor	34
9	Nitrobenzene	g-C$_3$N$_4$ (d_{50} ≈ 8–10 μm)	Azoxybenzene, azobenzene, and aniline	PFA capillary microreactor (d_c = 1.6 mm, L = 14.9 m)	Slurry: g-C$_3$N$_4$ (typically 5 mg/mL) suspended in the reaction mixture (8 mM nitrobenzene and 10 mM potassium hydroxide in 2-propanol. Gas: N$_2$, gas fraction from 0.2–0.9. Light: 405 nm LED (50–150 W); 20–60 °C	88% nitrobenzene conversion within 7.5 min at 50 °C, with 11% azoxybenzene selectivity, 68% azobenzene selectivity, and 4% aniline selectivity, compared with 93% conversion in batch reactor in 90 min	95

Table 2. continued

Entry	Substrate	Catalyst[a]	Product	Reactor[b]	Reaction conditions[c]	Results and advantages of flow operation	Ref
10	Ethanol	Au/TiO$_2$	H$_2$	Quartz microreactor (with 28 square microchannels, d_c = 500 μm, L = 10.5 cm)	Slurry: ethanol–water (1:9 molar ratio) with suspended Au/TiO$_2$ catalyst (0.02–0.44 mg/mL). Gas: air. Light: 365 nm UV LED (under irradiance of 1.93 and 3.86 mW/cm^2); ambient conditions	H$_2$ photoproduction rate increased with the photocatalyst loading up to 0.2 mg/mL, but decreased at higher loadings possibly due to particle agglomeration that influenced the light absorption or scattering; ~3.5 times higher photoproduction rate in wall-coated microreactors than that with the best slurry configuration in microreactors under similar operation conditions	97
11	4-(Trifluoromethyl)benzyl alcohol	TiO$_2$ (d_p ≈ 3.8 μm)	4-(Trifluoromethyl)benzaldehyde	Glass capillary milli-reactor (coupled with an ultrasound transducer, d_c = 2.2 mm, volume of 12.88 mL)	Slurry: 4-(trifluoromethyl)benzyl alcohol (1–5 mM) in acetonitrile with suspended TiO$_2$ (5 or 10 mg/mL). Gas: O$_2$. Light: 365 nm UV-A LED (64.8 W); 22.6–31.4 °C	The alcohol conversion (at 1 mM substrate and 5 mg/mL photocatalyst loading) under no ultrasound decreased from 57% in 14 min to 24% in 55 min, due to particle sedimentation upstream reducing the effective reactor volume; conversion improved under ultrasonic irradiation (e.g., 3.6 times), due to ultrasound providing better recirculation of photocatalyst and breakup of agglomerates	96
12	Methylene blue (MB)	Pd/SiO$_2$ (d_p = 40 μm)	Leuco-MB	PDMS microreactor with three parallel channels (square, d_c = 250 μm, separated by 50 μm thick walls)	Liquid: fluorinated FC-40 oil. Slurry: single Pd/SiO$_2$ particles encapsulated in droplets of ethanol containing 20 ppm MB. Gas: H$_2$ (flowing in the two gas channels and diffused to the reaction channel through walls); ambient conditions	The hydrogenation reaction completed in ~8 s; the microreactor system useful for single particle catalyst diagnostics in a multiphase reaction	98
13	Anisole	Zeolite catalyst (Y720, Y760 and Beta; d_p = 8–10 μm)	4-Metoxyacetophenone	PFA capillary milli-reactor (d_t = 2.2 mm)	Continuous phase: fluorinated oil. Slurry (as droplet): anisole with suspended zeolite catalyst (1 wt % loading), then mixed with acetic anhydride (1:3.5 molar ratio to anisole); 90 or 120 °C	~10–30% yields of 4-metoxyacetophenone in about 40 min for the three catalysts (with Y720 giving the best yield); reaction under kinetic operation due to sufficient and renewed contact between the catalyst and reactants	83
14	m-Nitrotoluene	10 wt % Pd/C	m-toluidine	PTFE capillary micro-reactor (d_t = 1.6 mm, L = 20 m)	Liquid (as droplet): 11 M aqueous potassium formate solution. Continuous slurry phase: Pd/C catalyst (2–8 g/L loading) suspended in toluene (containing m-nitrotoluene); 70 °C	80% m-nitrotoluene conversion in 35 min at 4 g/L catalyst loading; reaction hindered by incomplete circulation/mixing in the slug	82

^{a}d_p (mean) particle size; d_{10} or d_{50} denotes that 10% or 50% of particles are smaller than this size value; CMB-C$_3$N$_4$, modified carbon nitride; mpg-C$_3$N$_4$, mesoporous graphite carbon nitride; g-C$_3$N$_4$, graphitic carbon nitride. ^{b}d_c, inner (hydraulic) diameter of the (micro)reactor; L, reactor length; PTFE, polytetrafluoroethylene; PFA, polyfluoroalkoxy; FEP, fluorinated ethylene propylene; PDMS, polydimethylsiloxane. ^{c}[Bmim]BF$_4$, 1-butyl-3-methylimidazolium tetrafluoroborate.
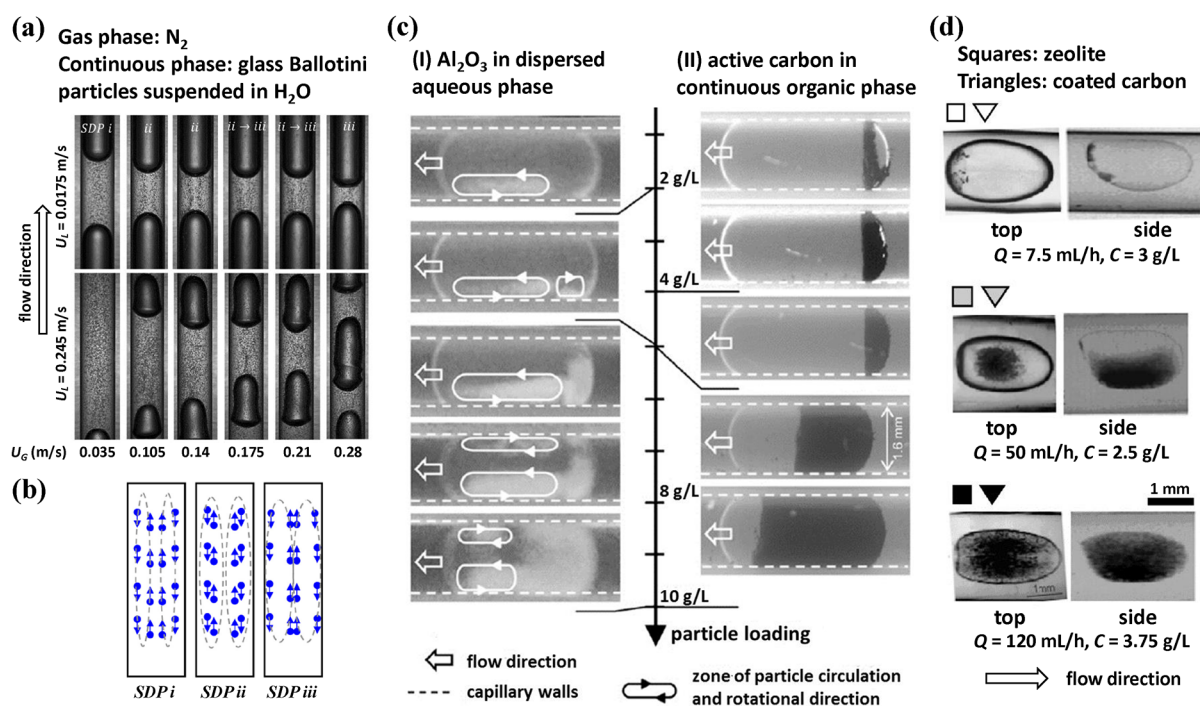
Figure 5. Liquid slugs and distribution of solid particles under different flow conditions in the microchannel (a); schematic description of three solid distribution patterns based on the real-time solid motion observed in experiments for superficial liquid velocity (U_L) = 0.0175 m/s (b); pictures of the particle distribution in the dispersed (water or aqueous potassium formate solution) or continuous organic (nitrotoluene dissolved in toluene) phase at different solid loadings (c) and in the dispersed ethanol phase (fluorinated oil as the continuous phase) at different total flow rates (Q) and solid loadings (C) (d). Parts a and b, c, and d were adapted with permission from refs 81, 82, and 83, respectively. Copyright 2021, 2011, and 2013 Elsevier.

2.3. Slurry in Microreactors. Slurry catalysts, prepared by suspending microscale catalyst particles into a mobile fluid phase (e.g., the reaction solvent) with a typical solid content below 25 mg/mL, have been combined with different flow operations in microreactors in various (photo)catalytic reaction applications such as hydrogenation, oxidation, fluorination, polymerization, and reduction reactions (Table 2).

2.3.1. Hydrodynamic Characteristics. For solid-catalyzed gas–liquid reactions, an attractive flow pattern is triphasic slug flow, where the slurry phase is the continuous phase separated by the dispersed gas bubbles (e.g., of H_2 or oxygen) (see Figure 1d). The slug flow characteristics and solid particle distribution in the slurry in microreactors have recently been critically reviewed by Peng et al.[76] The stability of the suspension is jointly determined by parameters such as particle size and surface properties, liquid medium properties (e.g., viscosity), and operating conditions (e.g., slug/bubble velocities).[77] Fine solid particles (e.g., 1 μm size) could be uniformly dispersed in the slug flow, while larger particles (e.g., 38 μm size) did not circulate and settled near the rear of the slug under the same conditions.

Particles can remain suspended in the same slug, fall through the liquid film between the bubble and microreactor wall (i.e., in the case of a wetting liquid phase), and travel among different liquid slugs, which can be explained using a theoretical model based on the force balance analysis of particles.[78] Under a given particle size, a critical capillary number or particle density exists for the particle to fall into the liquid film. Particles with more hydrophobic surfaces (i.e., in the aqueous slug) are more prone to be settled into the liquid

film under a specified particle size and capillary number. Besides, introducing particles in the liquid phase increases the liquid viscosity, leading to the decrease of the bubble detachment time at the microreactor inlet and of the formed bubble length.[79]

The velocities of the liquid–solid slurry (V_{L+S}) and the gas phase (V_G) also affect the solid distribution. At a low range of V_{L+S}, three different solid distribution patterns (SDP) were observed with increasing superficial gas velocity (U_G), namely particles distributed in the central region of the slug (SDP i), trapped inside the liquid circulation (SDP ii), and distributed at the edges of the liquid circulation (SDP iii) (Figure 5a and b).[76,80,81] On the other hand, it was demonstrated experimentally that adding solid (catalyst) particles in the liquid slug had a negligible effect on the slug velocity profile under lower gas (N_2) and slurry velocities (e.g., 0.002 or 0.004 m/s).[34] The solid charge in each slug was visually homogeneous, being mainly circulated in the lower part of the slug, despite the turbulence and vortex observed around the particle. At a high range of V_{L+S}, the slurry film was thick and more particles were observed in the film with the increase of V_G, which resulted in the bubble surface becoming more distorted (Figure 5a).[81]

For applications involving two immiscible liquid phases (e.g., biphasic reactions or reactions in droplets inside another inert carrier), solid catalysts can be suspended in either the dispersed droplet (Figure 1c) or the continuous slug (Figure 1d) phase of the liquid–liquid slug flow.

With solid particles in the dispersed phase through horizontal microchannels, depending on the properties of the liquid–liquid system (e.g., velocity and viscosity), the
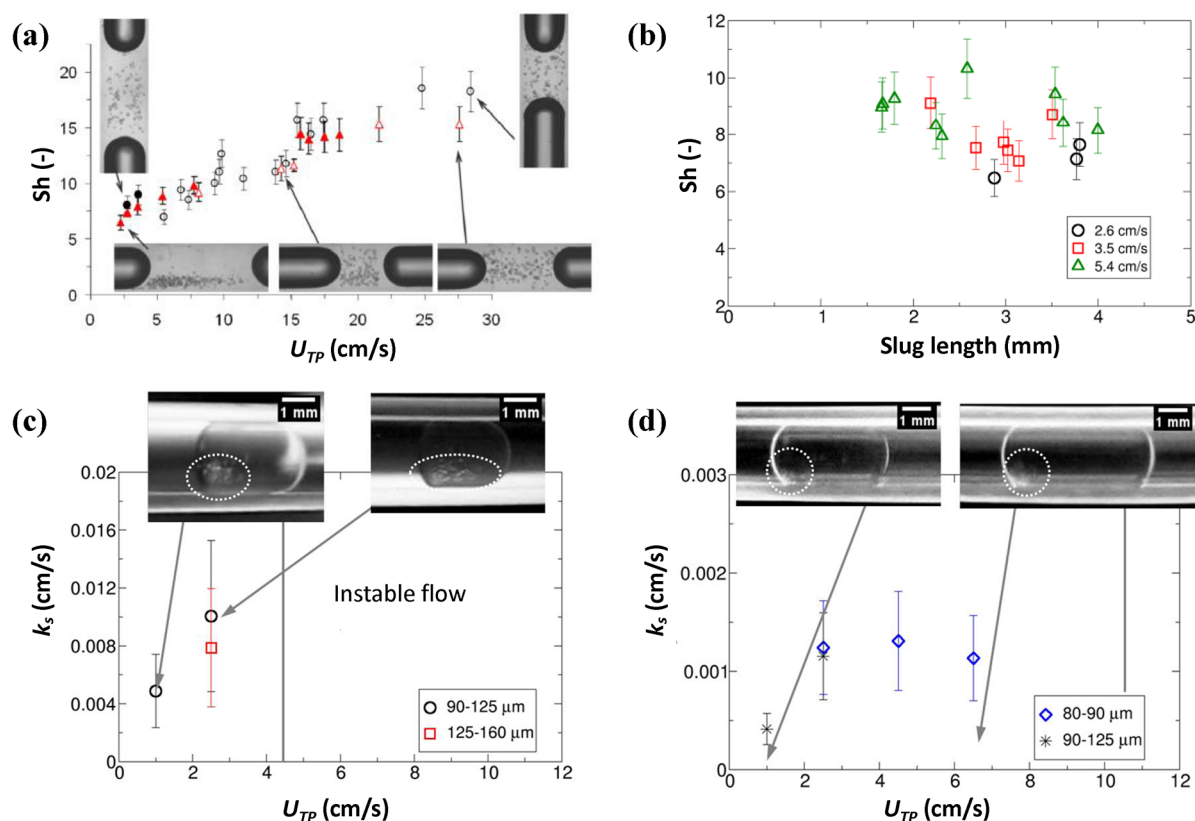
Figure 6. Influence of the two-phase velocity (U_{TP}) (a) and slug length (b) on the Sherwood numbers (Sh) for the nitrogen−aqueous−solid slurry slug flow in microreactors, with water/ethanol or water/acetonitrile as the liquid phase. Measured liquid−solid mass transfer coefficient (k_s) for aqueous−hexanol−solid (c) and aqueous−toluene−solid (d) slurry slug flows in microreactors. Cation exchange beads as particles were suspended in the aqueous phase in parts a−d. Part a was adapted with permission from ref 84. Copyright 2016 Elsevier. Parts b−d were adapted with permission from ref 85. Copyright 2015 ACS Publications.

circulation of solid particles was usually observed in the anterior section of the droplet, with more solids staying in the lower part especially if the solid has a much larger density than the dispersed liquid (Figure 5c).[82] In addition, counter-rotating vortices in the posterior section of the droplet were observed at high droplet velocities. However, high solid loadings would lead to a stagnant and extended posterior section, reducing the size of the anterior circulation section. This is supplemented by the work of Olivon and Sarrazin,[83] where three regimes for the suspension of (catalyst) particles were observed. At low flow rates, particles were stuck near the liquid−liquid interface (e.g., at the back of the droplet). Particles were better dispersed inside the droplet at intermediate flow rates, but still with a partial sedimentation at the bottom. Eventually, good homogenization could be achieved at high flow rates (Figure 5d). The transition between each dispersion state could be roughly rationalized via comparing the durations needed for the particle sedimentation and suspension via the flow-induced recirculation.

With solid particles in the continuous slug phase, Ufer et al.[82] observed an asymptotic and stable particle flow pattern (Figure 5c). An agglomeration of hydrophobic particles was found at the rear end of the aqueous droplet cap (i.e., the front of the organic slug), with a gradual extension into the organic wall film at higher solid loadings, despite a fraction of particles still remaining suspended in the slug by the inner circulation. This agglomeration was likely associated with the slug flow formation process in the vertical T-mixer used, where particles

in the organic phase (momentarily blocked in the upper capillary) could precipitate on the rear area of the emerging droplet.

2.3.2. Mass Transfer. Given the small particle size (e.g., 1−10 μm) and the mobile nature of the slurry catalyst in microreactors, an improved (external and internal) mass transfer is excepted compared with that in packed bed microreactors. This offers great opportunities for slurry-based microreactors in performing solid-catalyzed multiphase (gas−liquid or liquid−liquid) reactions which are usually hindered more by mass transfer than heat transfer.

For a gas−liquid−solid slurry slug flow in microreactors, the measured liquid−solid (L-S) mass transfer coefficient, expressed in the dimensionless form of Sherwood numbers (Sh), was found to increase when increasing the two-phase velocity (U_{TP}) from 2.2 to 16 cm/s (Figure 6a).[84] However, the Sh value had an only slight change at U_{TP} > 16 cm/s (being roughly the minimal velocity to achieve a homogeneous particle distribution in horizontal microreactors), the reason for which is still unclear. The flow orientation (vertical and horizontal) exerted no obvious influence on the L-S mass transfer coefficient, despite the fact that it influenced the particle distribution in the continuous slug. This suggests that the L-S mass transfer is only slightly affected by the particle dispersion, provided that particles are kept in motion and more or less homogeneously suspended. The increase of the solid loading (i.e., from 6 to 17 g/L) and mean particle size also showed little effect on the L-S mass transfer in microreactors,
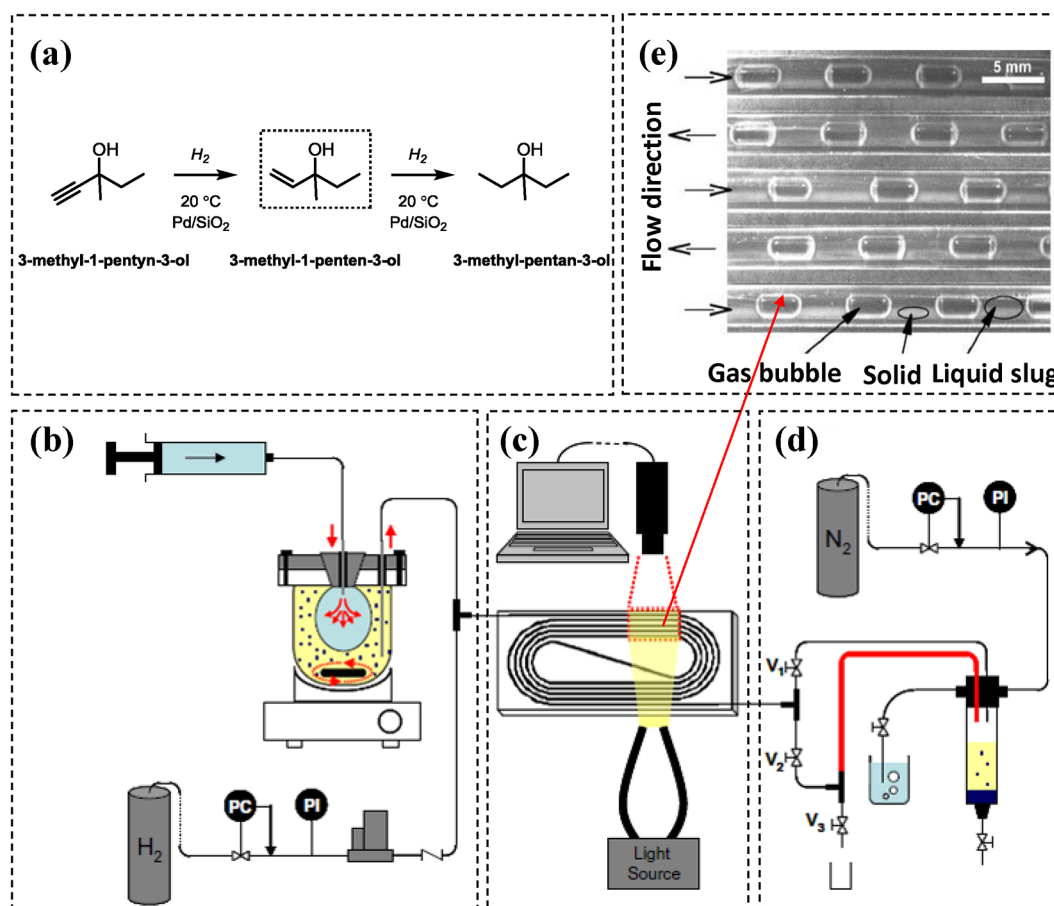
Figure 7. Gas−liquid hydrogenation of 3-methyl-1-pentyn-3-ol to 3-methyl-1-penten-3-ol under slurry catalysis in microreactors. (a) Reaction scheme. (b−e) Experimental setup used for slurry slug flow, including the injection zone for the gas and liquid−solid suspension (b), reaction and visualization zone (c), back pressure regulation and sample collection zone (d), and picture of the typical gas−liquid−solid slug flow obtained for a N_2/water system with 6.0 g/L of 100 μm Al_2O_3 particles in suspension (flow velocity of 3.6 cm/s) (e). Adapted with permission from ref 31. Copyright 2013 Elsevier.

possibly due to the still undisturbed particle circulation in the slug and somewhat negligible particle sedimentation given the relatively high velocity ranges studied. These results allowed development of the empirical *Sh* correlation in such micro-reactors, based on which the mass transfer performance of microreactors was compared with conventional counterparts (e.g., stirred tanks and bubble columns). The comparison results indicate that the triphasic slurry slug flow in microreactors can not only provide a comparable and good external mass transfer but also offer quasi ideal plug flow behavior attractive for reaction operations. Moreover, the L-S mass transfer coefficient under certain two-phase velocities in such microreactors was found to be independent of the slug length (Figure 6b).[85]

For a liquid−liquid−solid slurry slug flow in microreactors, the L-S mass transfer coefficient was found to depend mainly on the two-phase velocity, particle size, and circulation of solid particles in the liquid phase.[85] For example, with U_{TP} increased from 1 to 2.5 cm/s, the L-S mass transfer coefficient increased from 0.005 to 0.01 cm/s in aqueous−hexanol flow, and the used resin particles (d_p = 90−160 μm) accumulated somewhat in the rear end of the aqueous droplet (Figure 6c). In contrast, the L-S mass transfer coefficients were very small (e.g., 0.0013 cm/s) in aqueous−toluene flow under a U_{TP} of 1−6 cm/s velocity, and the resin particles (d_p = 80−125 μm) were

entirely segregated in the lower rear cap of the aqueous droplet (Figure 6d), possibly due to the (significant) particle agglomeration that slowed down the internal diffusion.

The gas−liquid mass transfer is also improved under the gas−liquid−solid slurry slug flow in microreactors. The absorption of CO_2 in water was shown to be enhanced by a factor of 1.43−2.15 via the addition of activated carbon particles (d_p = 1.96 μm), which is attributed to the shuttle mechanism.[86] A model was developed to relate the gas−liquid mass transfer enhancement factor (*E*) to parameters such as the adsorptive capacity of particles (*m*) and the coverage fraction of particles at the gas−liquid interface (ζ). The increase rate of *E* was fast at first; then, it slowed down with the increase of *m*. The addition of fine particles (meaning large ζ) can increase the apparent liquid viscosity, thus decreasing the mass transfer contribution by the shuttle mechanism, under which conditions *E* becomes constant. This model can provide a reasonable agreement with the experimental results; however, it neglects the solid particle properties at the gas−liquid interface (e.g., particle holdup and distribution).

The use of magnetic microparticles provides another strategy for actively controlling the liquid−solid mass transfer. The trajectory of particles could be controlled by the external magnetic field, e.g., to be in an oscillation movement orthogonal to the axial flow. This way, the fluid over the

microchannel cross section could be spanned by particles, resulting in the reduced diffusion length and enhanced liquid–solid mass transfer.[87] The liquid–solid mass transfer is also affected by periodical changes in the particle velocity induced by the applied magnetic field. According to the simulation in the case of a fast chemical reaction on the surface of catalytic magnetic microparticles placed in laminar flow microreactors, the liquid–solid mass transfer coefficient could be reduced up to 7.6% by the periodic particle movement with different particle velocities, when compared with that under steady state motion with the same mean velocity.[88] Thus, a further optimization of magnetic actuation is necessary to maximize the mass transfer rate.

2.3.3. Reaction Application Examples. An extensive collection of examples about the application of slurry catalysts for reactions in microreactors as well as some examples for millireactors is listed in Table 2, including catalytic reactions such as (transfer) hydrogenation, oxidation, and Friedel–Crafts reactions (entries 1–6 and 12–14) and photocatalytic reactions such as fluorination, polymerization, reduction, dehydrogenation, and oxidation reactions (entries 7–11). Very recently, Peng et al.[76] also discussed the application of slurry in microreactors for uses in, for example, crystallization, synthesis of fine particles, and some catalytic reactions.

A notable application of slurry catalysts in microreactors was reported by Liedtke et al.[31] for the gas–liquid hydrogenation of 3-methyl-1-pentyn-3-ol to 3-methyl-1-penten-3-ol (as an important intermediate for manufacturing fine chemicals) (Figure 7a; Table 2, entry 1). The catalyst (5 wt % Pd/SiO$_2$ with a mean particle size of 40 μm) was suspended in the reaction solvent (ethanol) under stirring, and the formed slurry was pushed into the PFA capillary microreactor (d_c = 1.65 mm) to merge with H$_2$ to form a stable gas–liquid–solid slug flow (Figure 7b–e). The experimental specific pressure drop gradient was 1.1–2.1 kPa/m with the increase of gas flow rate (14–30 N mL/min) under a 3 mL/min slurry flow rate. The conversion of 3-methyl-1-pentyn-3-ol reached about 90% in 150 s at 20 °C, with the selectivity of 3-methyl-1-penten-3-ol close to 1 (due to using quinoline as the modifier to avoid its successive hydrogenation to 3-methyl-pentan-3-ol). Under this temperature, the substrate conversion profile in the microreactor matched that obtained in a well-stirred batch reactor in which reaction was proven under the kinetic regime. This supports the overall high mass transfer rate achieved under such gas–liquid–solid slug flow operation for this fast reaction.

The beneficial gas–liquid hydrogenation over slurry catalysts has also been demonstrated in Corning advanced-flow microreactors with the hydraulic diameter of fluidic channels around 1 mm.[89–91] The enhanced heat and mass transfer in microreactors enabled a drastic reduction of the required reaction time for the desired conversion to below 2 min (versus >10 h in batch), as shown for the highly exothermic hydrogenation of a pharmaceutical compound over a noble metal slurry catalyst.[90] Furthermore, the slurry hydrogenation of ethyl cinnamate to ethyl 3-phenylpropanoate (as a pharmaceutical intermediate or used in organic synthesis) in this type of microreactor was tested.[91] Using the commercial Pd/C catalyst in a stable slurry form (in ethanol), a high yield (98%) of ethyl 3-phenylpropanoate was obtained in the microreactor at 75 °C in 18 s, corresponding to a productivity of 51.3 g/h (in contrast to 27.8 g/h at 25 °C) (Table 2, entry 2). However, the yield decreased to 93% in 30 s, which was ascribed to the nonoptimal mixing of the gas–liquid–slurry

mixture leading to lower heat/mass transfer rates. Similar intensification potentials of slurry catalysis in flow have been shown in earlier research reports of Enache and co-workers in millireactors as well as microstructured (heat exchange) reactors for gas–liquid hydrogenation reactions (of isophorone or resorcinol over, e.g., Pd/C catalyst) and oxidation reactions (of glycerol over Au/C catalyst) (Table 2, entries 3–6).[21,92–94] For example, the hydrogenation of isophorone to trimethyl cyclohexanone over the slurry catalyst of Pd/C in a capillary reactor (d_c = 3.86 mm) yielded a reaction rate increase of 5–8 times at 60–100 °C compared with the batch autoclave system (Table 2, entry 4), due to the enhanced mass transfer in flow that enabled the reaction to be actually operated under kinetic control.[21] However, in all the above-mentioned research no specific data about the gas–liquid–slurry hydrodynamics were provided (e.g., regarding the flow stability and flow regime inner details though it seemed that slug flow likely prevailed under a range of conditions), hampering a more in-depth reactor performance analysis.

The slurry catalyst within a gas–liquid–solid slug flow has been further utilized to achieve more efficient photocatalysis in microreactors as well as millireactors.[33,34,95,96] The first type of applications in this respect deals with the use of an inert gas phase to enhance the liquid–solid slurry mixing and thereby the photocatalytic performance. In the work of Pieber et al.,[33] the photocatalyst (i.e., a modified carbon nitride, CMB-C$_3$N$_4$) was suspended in the viscous 1-butyl-3-methylimidazolium tetrafluoroborate ([Bmim]BF$_4$)–water mixture to suppress its settling. The stable catalyst suspension was dosed into a gas–liquid slug flow of nitrogen and the reaction solvent (acetone/acetonitrile–water mixture) in a FEP (fluorinated ethylene propylene) capillary microreactor (d_c = 1.6 mm). As such, similar amounts of CMB-C$_3$N$_4$ were homogeneously distributed in each liquid slug by its interior vortices and, therefore, uniformly irradiated by the 420 nm LED array. The photocatalytic microreactor system was demonstrated among others for the decarboxylative fluorination of phenoxyacetic acid using selectfluor (Table 2, entry 7). A quantitative yield (94%) of fluoromethoxyenzene as the monofluorinated product was obtained in a residence time of 14 min. Moreover, for this reaction the generated CO$_2$ could easily desorb from the liquid slug to the gas bubble without (much) disturbing the flow integrity. A three-step filtration–extraction protocol allowed the desired product isolation and recovery of the catalyst and the suspension solvent [Bmim]BF$_4$. When using the homogeneous Ru[bipy]$_3$Cl$_2$ photocatalyst in the microreactor, the desired product yield was lower, accompanied by the reactor fouling of a solid material (assumed by the decomposition of Ru[bipy]$_3$Cl$_2$) that seriously disrupted an otherwise regular gas–liquid slug flow. This confirms the better performance of the heterogeneous CMB-C$_3$N$_4$ photocatalyst and triphasic slug flow using slurry catalysts.

Such inert-gas-assisted liquid–solid photocatalytic reaction under triphasic slug flow was also applied for PET-RAFT (photoinduced electron/energy transfer reversible addition–fragmentation chain transfer) polymerization of methyl methacrylate (MMA) in a PFA capillary microreactor (d_c = 1.6 mm) (Table 2, entry 8).[34] The slurry was prepared by adding mesoporous graphite carbon nitride catalysts (mpg-C$_3$N$_4$; d_p ≈ 5 μm) into the reactant liquid (MMA as the monomer, 4-cyano-4-(dodecylsulfanylthiocarbonyl)-sulfanyl-pentanoic acid as the RAFT agent, triethanolamine as the reducing agent, and dimethyl sulfoxide as the solvent) (Figure
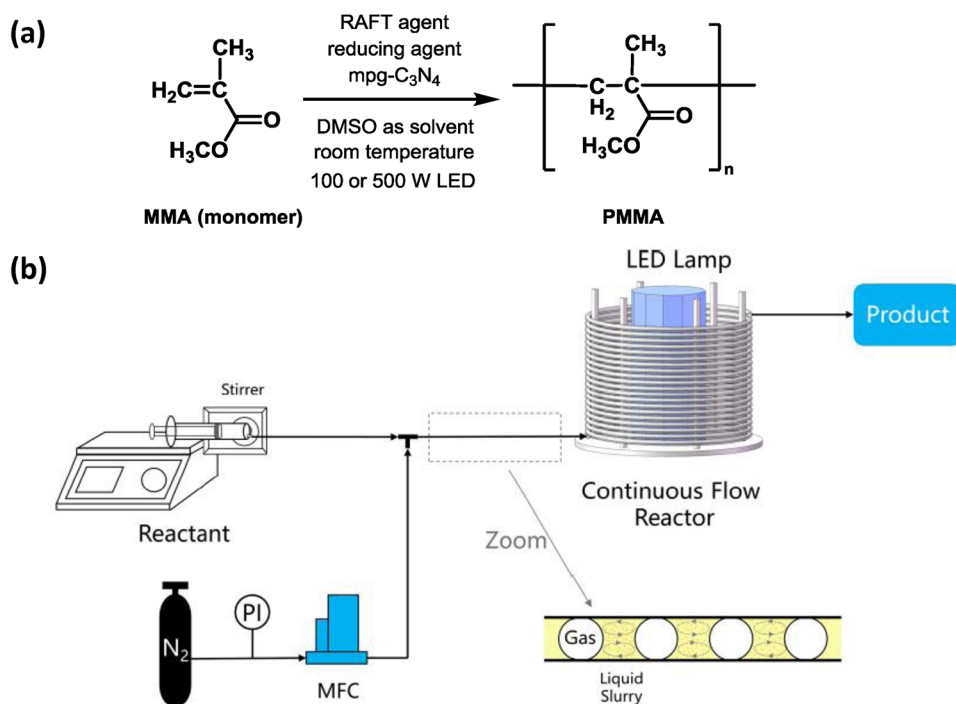
Figure 8. PET-RAFT polymerization of MMA in the microreactor. (a) Reaction scheme. (b) Schematic diagram of the continuous gas–liquid–solid slug flow microreactor setup. Adapted with permission from ref 34. Copyright 2021 ACS Publications.
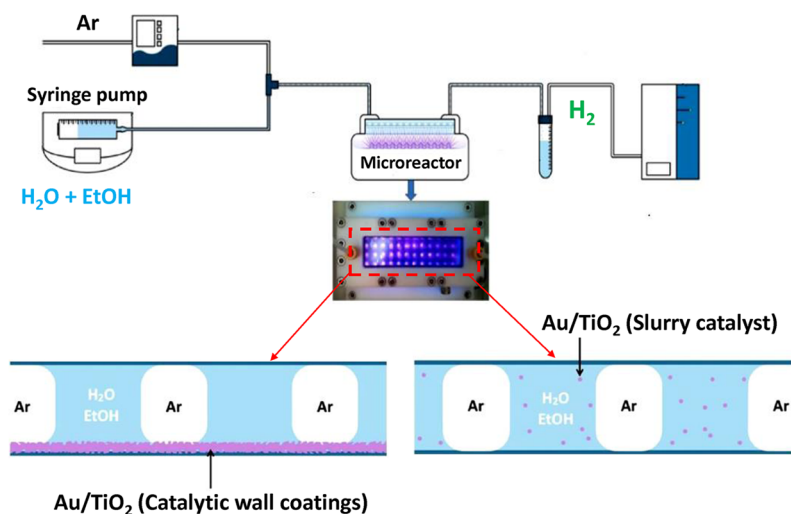

Figure 9. Photocatalytic hydrogen generation in microreactors with catalytic wall coatings and slurry catalyst. Adapted with permission from ref 97. Copyright 2020 Elsevier.

8a). N_2 was added to create a gas–liquid–solid slug flow that could well stir the solid photocatalyst by recirculation in the liquid slug (Figure 8b). Under a UV LED light irradiation at 500 W, the apparent rate constant for MMA polymerization in the gas–liquid–solid slug flow is ca. 2 times higher than that in a batch reactor (10 mL test tube), showing the better light penetration through slurries in the microreactor. The MMA conversion in the microreactor increased from 19% to 46% when the catalyst loading changed from 0 to 0.5 mg/mL in 100 min and slightly decreased when further increasing the loading to 3 mg/mL. This phenomenon was explained by the blocked light transmission caused by the excess photocatalyst suspended in the liquid slug. Besides, the mpg-C_3N_4 catalyst in the triphasic flow could be recycled (by filtering and then

washing and drying) and reused five times, showing a stable polymerization rate.

Another example was demonstrated by the same group in the photocatalytic reduction of nitrobenzene to azo-compounds (azoxybenzene and azobenzene as important precursors in, e.g., the pigment and pharmaceutical industries), using the slurry catalyst of graphitic carbon nitride ($d_p \approx 10$ μm) and inert N_2 within a gas–liquid–sold slug flow through the PFA capillary microreactor ($d_c = 1.6$ mm) (Table 2, entry 9).[95] Under illumination by a blue LED light source, the nitrobenzene conversion could achieve 88% within 7.5 min at 50 °C, with the selectivities to azoxybenzene and azobenzene being 11% and 68%, respectively. In comparison, 90 min was needed for a comparable conversion (93%) in the batch
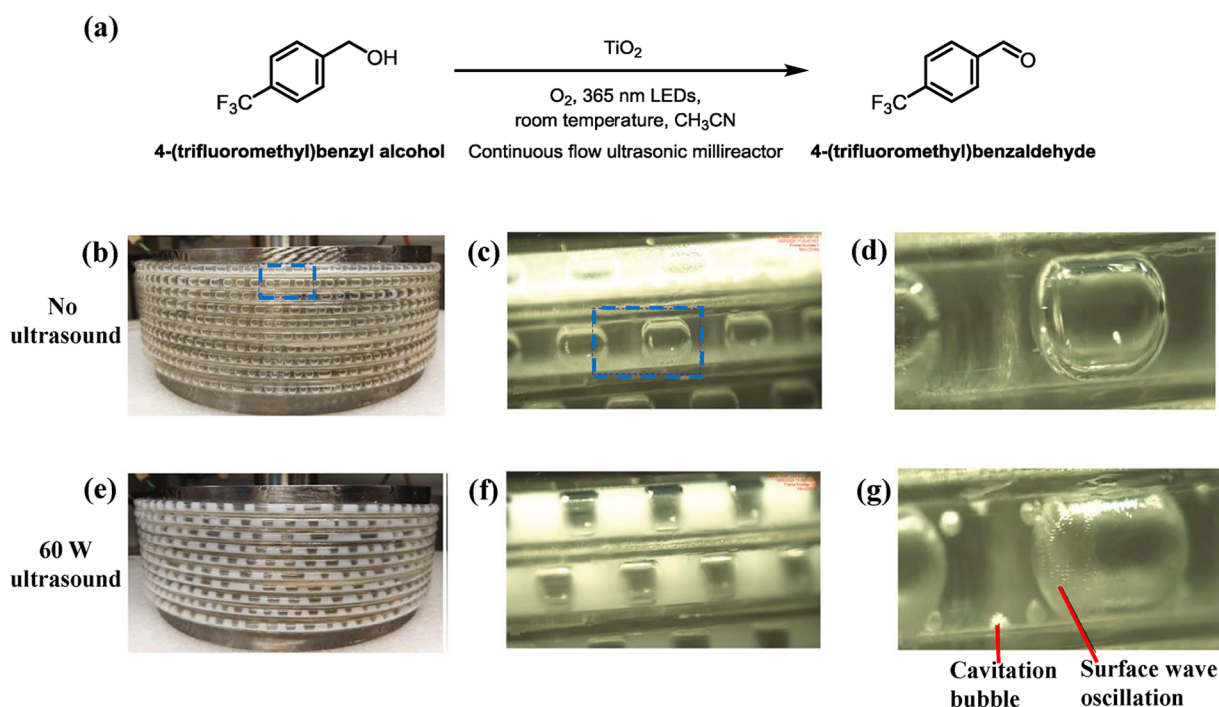
Figure 10. Photocatalytic oxidation of 4-(trifluoromethyl)benzyl alcohol in a glass capillary millireactor. (a) Reaction scheme. (b−d) Performance of gas−liquid−solid slug flow without ultrasound and (e−g) with ultrasound. Parts b and e are the full view of the reactor (flow rate was 1 mL/min for both the gas and liquid slurry phase containing 10 g/L TiO$_2$). Parts c and f are the zoomed views of the first three spirals of the capillary. Parts d and g are the zoomed views of a section of the second spiral, where the flow rates were 0.8 and 0.6 mL/min for the gas and slurry phase, respectively. Adapted with permission from ref 96. Copyright 2022 Elsevier.

reactor due to a much worse light penetration. An optimal catalyst loading was found at 5 mg/mL, beyond which the reaction rate in the microreactor decreased due to a quick light decay within the catalyst slurry, consistent with the PET-RAFT polymerization case.[34] Furthermore, the reaction rate was improved at a relatively high gas fraction (0.67) and increasing flow rate, which was explained by the enhanced mass transfer between the catalyst and reactants in the (shortened) liquid segment and the increased thickness of the liquid film around bubbles to help receive more photons.

Recently, the activity of microreactors with the slurry catalyst and catalytic wall coatings in the photogeneration of hydrogen from the water−ethanol mixture has been studied (Table 2, entry 10).[97] Au/TiO$_2$ photocatalyst was either dispersed in the reaction mixture or coated onto the quartz microreactor wall (Figure 9), with the inert Ar carrier gas being used to create a gas−liquid(−solid) slug flow and facilitate the transfer of hydrogen from liquid to gas. Under UV irradiation, the photoactivity in terms of the hydrogen production rate (i.e., via ethanol dehydrogenation) based on the photocatalyst amount was found to be ∼3.5 times higher in the coating configuration than the slurry configuration, due to the opacity of the slurry (especially at high catalyst loadings) that tended to limit the photon transfer. Thus, to unlock the full potential of the slurry configuration in microreactors for efficient photocatalysis, more research including the proper reaction system selection and operation parameter optimization thereof is further required.

The second type of photocatalytic applications concerns the presence of gas-phase reactant and slurry catalyst in a triphasic slug flow. This has been demonstrated for the photocatalytic oxidation of 4-(trifluoromethyl)benzyl alcohol to 4-(trifluoromethyl)benzaldehyde using molecular oxygen and TiO$_2$ photocatalyst in a glass capillary millireactor (d_c = 2.2 mm) under UV-A irradiation (Figure 10; Table 2, entry 11).[96] The slurry of TiO$_2$ powders (d_p ≈ 3.8 μm) dispersed in the alcohol reactant−acetonitrile mixture merged with O$_2$ forming a gas−liquid−solid slug flow in the capillary. To realize a good catalyst suspension, the reactor was coupled with ultrasound (i.e., by wrapping the capillary around an irradiating cylinder connected with a sonotrode and a Langevin-type transducer). Applying ultrasound proved to have a pronounced and positive effect on the slurry flow stability and reaction efficiency. Without ultrasound, a quick sedimentation of TiO$_2$ particles occurred at the (very) upstream of the capillary, leading to a gradual decrease of the particle amounts present along the reactor length (Figure 10b−d). Accordingly, the alcohol conversion decreased from 57% to 24% when increasing the residence time from 14 to 55 min (at 1 mM alcohol concentration and 5 mg/mL catalyst loading at approximately room temperature), since the particle settled in a smaller fraction of the reactor length reducing the effective reactor volume with a good particle suspension. The particles were resuspended within seconds after applying ultrasound, which was caused by the enhanced mixing from the generated cavitation bubbles and surface wave oscillation of the oxygen bubbles (Figure 10e and f). As a result, the alcohol conversion was much improved with ultrasound (e.g., maximum being 3.6 times) due to the better exposure of particles to the light, and the conversion logically increased from 71% to 86% upon raising the residence time from 14 to 28 min. In both scenarios, 4-(trifluoromethyl)benzyl alcohol was found as the main product, with the selectivity being around 95% or 85% at conversions below 40% or above 60%.
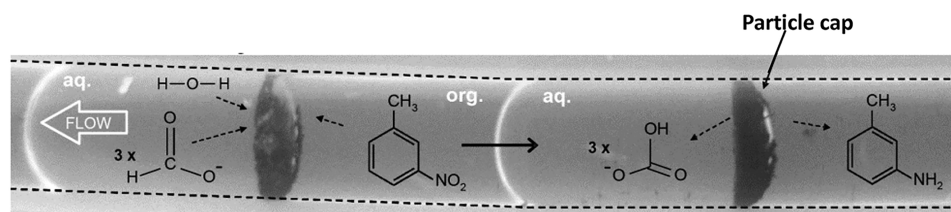
Figure 11. Schematic of the catalytic transfer hydrogenation of *m*-nitrotoluene within a liquid−liquid−solid slug flow in the microreactor. Pd/C catalyst (4 g/L) in the wall-wetting organic toluene phase was seen to form a contiguous cap around the dispersed aqueous slug. Reproduced with permission from ref 32. Copyright 2011 Wiley.

Slurry catalysts have also been suspended in droplets of the reactant−solvent mixture in (micro)flow, using an additional immiscible liquid carrier, for catalyzing liquid-phase or gas−liquid reactions.[83,98] Nieuwelink et al.[98] performed liquid-phase hydrogenation of methylene blue (MB) to Leuco-MB in a microreactor (Table 2, entry 12). The microreactor has three parallel channels separated by two 50 μm thick polydime-thylsiloxane (PDMS) walls with high H_2 permeability. A fluorinated hydrocarbon oil flowed in the middle reaction channel (d_c = 250 μm) as the inert continuous phase, with Pd/SiO_2 particles (d_p = 40 μm) encapsulated in droplets of ethanol containing 20 ppm MB, and H_2 diffused from the other two channels through the PDMS wall to facilitate the reaction. Droplets encapsulating single particles were formed, which are challenging to obtain due to fluctuating particle concentrations near the reactor inlet, allowing for diagnosing multiple catalyst particles. The preliminary results show that the fast hydrogenation of MB to Leuco-MB only needed approximately 8 s to complete in the microreactor, as visualized by the discoloration of catalyst particles in ethanol droplets. The acylation of anisole as an industrially relevant reaction was also investigated in a PFA capillary millireactor (d_c = 2.2 mm) over slurry catalysts (Table 2, entry 13).[83] The slurry was prepared by dispersing zeolite (such as Y720, Y760, and Beta; d_p = 8−10 μm) in pure anisole and then mixed with the other reactant (acetic anhydride) in the reactor and traveled down as droplets carried by an inert fluorinated oil. Under such liquid−liquid−solid slug flow (e.g., Figure 1c), up to ∼10−30% yield of the product (4-metoxyacetophenone) was attained in about 40 min for the three catalysts studied in the millireactor. The yield profile for each catalyst compares well with that in a well-stirred batch reactor, showing the current flow system as a promising candidate for kinetic study and catalyst screening. Interestingly, the catalyst dispersion in the droplet was found to change from partial to good homogenization when increasing the flow rate as a result of competition between sedimentation and flow-induced recirculation. However, this suspension state difference did not influence the liquid-phase reaction kinetics obtained, suggesting that for this slow reaction, a sufficient catalyst−reactant contact was still ensured by convection in droplets even in the case of partial homogenization (e.g., particles preferentially located in the bottom hemisphere of droplets; see Figure 5d). Though the primary focus of these two research reports is on high-throughput catalyst screening,[83,98] they provide important insights into solid flow manipulation toward efficiency increase in (gas−)liquid−solid reactions under suspension catalysis in microreactors.

The principle of using suspension catalysis in microreactors for the liquid−liquid catalytic reaction has been demonstrated by Ufer et al.[32,82] The catalytic transfer hydrogenation of *m*-nitrotoluene (dissolved in toluene) with aqueous potassium formate to *m*-toluidine over 10 wt % Pd/C slurry catalyst was tested (Table 2, entry 14), which is a useful reaction type adopted toward the synthesis of specialty chemicals and pharmaceuticals. The catalyst particles suspended in the organic (toluene) phase flowed through a PTFE capillary microreactor (d_c = 1.6 mm) as the continuous slug. A prevailing liquid−liquid−solid slug flow pattern was found, with the catalyst particles accumulating around the rear cap end of the dispersed aqueous droplets and extending into the surrounding organic wall film (Figure 11). At 70 °C and residence times up to 35 min, the *m*-nitrotoluene conversion in the microreactor was found to be slightly lower than that obtained in a stirred tank reactor under identical reaction conditions, and the conversion difference was enlarged when lowering the flow rate. This was explained by the reaction rate under kinetic control in batch due to a (nearly) perfect mixing and large interfacial area generated by the high energy input, while in the microreactor, the reaction was hindered by the somewhat inadequate mass transfer, particularly due to the incomplete circulation in the slug at lower slug velocities,[32,82] indicating further room for optimization.

3. CHALLENGES AND FUTURE PERSPECTIVES

Though microreactors have been shown to greatly improve, among others, the reaction efficiency by operation with the continuous transport of solid (catalyst) particles, there are several major challenges to overcome in order to increase its technical feasibility and economic potential toward real industrial applications.

Solid handling is not trivial in microreactors. Fouling and even blockage can happen when particles have a chance to become in direct contact with the microreactor wall.[12] Moreover, the particle growth or sedimentation over time or under flow/reaction conditions can result in an inferior (catalytic) performance. Colloids are heterogeneous mixtures of two or more substances and, thus, have an insufficient stability period.[99] After a certain time, the dispersed nano-particles can settle from the continuous liquid phase and form two separate phases, which can have a negative effect on their properties or cause clogging of microreactors resulting in their performance deterioration.[53] Some physical (e.g., magnetic stirring and ultrasonification) and chemical (e.g., adding surfactants or polymers as capping agents) methods of treatment have been used to increase their stability;[36] still, long-term stability (e.g., over months) remains not easy to achieve, as it entails more dedicated colloidal suspension preparation procedures. Besides, there is another possible approach to improve the dispersion of solid particles in fluids. The manipulation of magnetic solid particles (e.g., ferrofluids) in flow can be better achieved by applying external magnetic

fields in addition to pressure-driven flow.[54−56] This also provides new possibilities for improving biphasic (gas−liquid, liquid−liquid, or liquid−solid) mass transfer and reaction in microreactors.[61,63,64] Moreover, the controlled synthesis of (catalyst) nanoparticles has been well explored in micro-reactors.[15] This, combined with their further uses in micro-reactors, offers an excellent opportunity for increasing the microreactor application potential.

For slurry catalysts using microparticles, the sedimentation in flow is even more visible given the larger particle size in the micrometer range. These uncertainties pose a threat to their wide and flexible application in microreactors. Coupling microreactors with ultrasonification or encapsulating particles in droplets seems to help mitigate the wall deposition.[83,96] Ultrasound was reported to assist crystallization or particle synthesis in microreactors,[100] for example, to obtain a small mean crystal size of adipic acid with a narrowed size distribution and high crystal production rate.[101] During ultrasonic irradiation, seeding is no longer needed to induce primary nucleation, because cavitation occurs which can promote crystal nucleation with better control.[102] Due to strong cavitation effects, ultrasound broke up the particle agglomerates, and the mean size and span of the synthetic particles (e.g., calcium carbonate) could be reduced by 1 order of magnitude by applying low-frequency ultrasound in microreactors.[103] Moreover, there was a steady pressure drop for a long operation time in the presence of ultrasound, which proved that ultrasound did prevent clogging. In contrast, the pressure drop increased rapidly in the liquid without applying ultrasound and reached up to 4.5 times higher.[104] Hence, ultrasound is envisaged as a promising method to improve the dispersion of solid catalysts in the slurry system in micro-reactors. A recent work showed that the photocatalytic microparticles (e.g., TiO_2) rapidly settled down in a gas−liquid−solid slug flow through millireactors without ultra-sound, whereas they were resuspended within a few seconds when ultrasound was applied.[96] The cavitation bubbles, acting as microstirrers, moved randomly and oscillated vigorously in the liquid slug to improve the particle dispersion. However, this cannot be easily adapted for all reaction systems without introducing further complexity of the setup or flow pattern. The improved transportation of particle-laden liquids has been shown in large-sized conduits through the creation of swirling flow patterns, e.g., using pipes with continuously varying cross sections[105] or attaching helical blades inside pipes.[106] The application of swirling flow intensified the turbulence motion, thus improving the dispersion of solid particles and minimizing the wear on the pipe walls and the pipe blockage.[107] Such turbulence motion enhanced the mixing of fluids and, hence, improved the mass transfer performance.[108−110] To induce such swirling flow in microreactors might provide another option to keep a good dispersion of solid (catalyst) particles in the liquid flow and enhance the liquid−solid mass transfer.

Another challenge is the recovery of catalyst from the flow (e.g., for reasons of catalyst deactivation or its reuse). Though a simple decantation was used to separate aqueous-based colloidal catalysts from the organic phase[20] or filtration/centrifugation could be applied to collect nano- or micro-particles at the microreactor outlet,[25,33] tedious procedures (done in batch) are often required to either isolate the product from the catalyst-containing liquid or regenerate the catalyst via thermal treatment. Ideally, these procedures should also be made in continuous flow in order to well match with

microreactor processing at high production capabilities.[49] In this regard, the use of magnetic (nano)particles as catalysts suspended in flow through microreactors may present an attractive alternative. They might be easily recycled out of the reaction medium with a magnetic field and reused without a (significant) reduction of catalytic performance as reported for reactions such as hydrogenation and oxidation in batch.[111,112]

The application of flowing PEs in microreactors remains a much less explored area,[30] and thus, ample opportunities are foreseen here. One major challenge in this area is to further improve the emulsion stability using nanoparticles that can be applied as both a highly active catalyst and stabilizer at the liquid−liquid interface under a variety of reaction conditions.[70] Research along this direction will expand reaction databases that can benefit from PE-based microreactor operation in a more efficient and sustainable manner. Besides, most research focuses on describing the stabilization mechanism of spherical solid particles while that of nonspherical particles is less known,[113] which could limit, to some extent, the choice of promising catalysts (or its support) and, thus, applications in microreactors. Moreover, performing reactions involving gas reactant (e.g., H_2 or O_2) in the presence of PEs could be another interesting area to explore in microreactors. In short, PEs still represent an emerging area with rarely reported catalytic applications in microreactors, which needs a joint effort from both chemists and chemical engineers.

Last but not least, scaleup of microreactors containing solid particles in flow to high production capacities that meet industrial needs is essential for technology implementation in practice. Strategies based on a numbering-up approach have been well studied for reaction systems involving pure liquids within a single-phase or multiphase flow.[114] To further handle particle flow in the upscaled microreactor system, these strategies might still be applicable with a further consideration of the local particle hydrodynamics.[32,49,76] The practical application of microreactors is being slowly integrated into the chemical industry, given their great potential for continuous flow chemistry and chemical synthesis. A pilot plant was established for heterogeneously catalyzed gas-phase reactions (epoxidation of propene to propene oxide with H_2O_2 in vapor form, over titanium silicalite catalysts coated on the microreactor wall).[115] Around 90% selectivity of propene could be obtained for a total period of more than 250 h, and a good catalyst stability was observed. Besides, the operation conditions were reproducible over a wide parameter range during all operation processes, proving the feasibility of the direct transfer from the lab scale into production on an industrial scale. The Corning advanced-flow reactor, as one well-known type of commercial milli- or microreactor based on glass, has different scale-up versions realized via the numbering-up and sizing-up strategies.[114,116,117] It has been shown to enable producing 1000 to 10,000 ton/year of active pharmaceutical ingredient (API) in the fine chemical and pharmaceutical industries.[89,114,118] These successful examples will certainly help pave the way for the future industrial application of microreactors containing solid particles in flow toward achieving efficient and more sustainable chemical conversions.

4. CONCLUSION

Manipulation of solid particle flow in microreactors provides great opportunities to perform (heterogeneously) catalyzed reactions in an efficient way. Compared with wall-coated or

packed bed microreactors, catalyst particles in microflow allow flexible production with a relative ease of catalyst recovery and, in the meantime, render a good or even better heat/mass transfer rate. Promising reaction applications utilizing the colloidal suspensions, PEs and catalyst slurries have been demonstrated in microreactors. Important examples include, among others, (gas–liquid or gas–liquid–liquid) hydrogenation, gas–liquid oxidation, inert-gas-assisted fluorination and polymerization, and biphasic liquid–liquid catalytic reactions, where solid particles are typically encapsulated as colloidal or slurry (photo)catalysts within either the dispersed droplet or the continuous slug or located at the liquid–liquid interface as the stabilizer of PE droplets. Significant intensification potential has been illustrated primarily thanks to the enhanced transfer (of matter and/or light) under such particle-laden flow processing in microreactors, which allowed obtainment of the maximized reaction rate (i.e., in the kinetic regime) or superior performance (in terms of the reaction conversion or product yield) compared with their batch counterparts. A further understanding of the reaction behavior in microreactors could be aided by the existing knowledge of particle hydrodynamics (e.g., solid distribution pattern and circulation in the droplet or slug) and the effect of particle dispersion state on (gas–liquid, liquid–liquid, and liquid–solid) mass transfer.

Despite these application advantages showcased in microreactors, there are still some challenges to overcome for their successful implementation in industrial practice. The long-term particle stability during flow processing in microreactors under reaction conditions has to be improved via, e.g., developing effective particle synthesis procedures, choice of a proper flow regime, or coupling with ultrasonification. More simplified procedures for the facile recovery of catalysts in flow and their subsequent reuse without performance loss also need to be developed. Scaling-up strategies with a consideration of local particle hydrodynamics in microreactors need to be further examined for the production capacity increase.

Numerous opportunities are envisaged for using microreactors with continuous flow of solid particles in other multiphase (photo)catalytic reactions, especially for the case of PEs, which remains a much less explored area. The fundamentals of the hydrodynamics and mass transfer of these solid-laden microflow systems also need to be further studied in great depth, in order to better elucidate the microreactor performance and help to unlock its full potential in chemical process intensification.

■ AUTHOR INFORMATION

Corresponding Author

Jun Yue − Department of Chemical Engineering, Engineering and Technology Institute Groningen, University of Groningen, 9747 AG Groningen, The Netherlands; orcid.org/0000-0003-4043-0737; Email: yue.jun@rug.nl

Author

Jie Zong − Department of Chemical Engineering, Engineering and Technology Institute Groningen, University of Groningen, 9747 AG Groningen, The Netherlands

Complete contact information is available at:
https://pubs.acs.org/10.1021/acs.iecr.2c00473

Notes

The authors declare no competing financial interest.

■ ACKNOWLEDGMENTS

■ REFERENCES

(1) Fanelli, F.; Parisi, G.; Degennaro, L.; Luisi, R. Contribution of microreactor technology and flow chemistry to the development of green and sustainable synthesis. *Beilstein J. Org. Chem.* **2017**, *13* (1), 520−542.

(2) Yue, J. Multiphase flow processing in microreactors combined with heterogeneous catalysis for efficient and sustainable chemical synthesis. *Catal. Today* **2018**, *308*, 3−19.

(3) Jahnisch, K.; Hessel, V.; Lowe, H.; Baerns, M. Chemistry in microstructured reactors. *Angew. Chem., Int. Ed. Engl.* **2004**, *43* (4), 406−446.

(4) Jensen, K. F. Flow chemistry-Microreaction technology comes of age. *AIChE J.* **2017**, *63* (3), 858−869.

(5) Plutschack, M. B.; Pieber, B.; Gilmore, K.; Seeberger, P. H. The Hitchhiker's guide to flow chemistry parallel. *Chem. Rev.* **2017**, *117* (18), 11796−11893.

(6) Yao, C.; Zhu, K.; Liu, Y.; Liu, H.; Jiao, F.; Chen, G. Intensified CO_2 absorption in a microchannel reactor under elevated pressures. *Chemical Engineering Journal* **2017**, *319*, 179−190.

(7) Wang, K.; Li, L.; Xie, P.; Luo, G. Liquid−liquid microflow reaction engineering. *Reaction Chemistry & Engineering* **2017**, *2* (5), 611−627.

(8) Gemoets, H. P.; Su, Y.; Shang, M.; Hessel, V.; Luque, R.; Noel, T. Liquid phase oxidation chemistry in continuous-flow microreactors. *Chem. Soc. Rev.* **2016**, *45* (1), 83−117.

(9) Hommes, A.; Disselhorst, B.; Yue, J. Aerobic oxidation of benzyl alcohol in a slug flow microreactor: Influence of liquid film wetting on mass transfer. *AIChE J.* **2020**, *66* (11), e17005.

(10) Mallia, C. J.; Baxendale, I. R. The use of gases in flow synthesis. *Org. Process Res. Dev.* **2016**, *20* (2), 327−360.

(11) Weeranoppanant, N. Enabling tools for continuous-flow biphasic liquid−liquid reaction. *Reaction Chemistry & Engineering* **2019**, *4* (2), 235−243.

(12) Wu, K.; Kuhn, S. Strategies for solids handling in microreactors. *Chim. Oggi* **2014**, *32* (2), 62−66.

(13) Ma, J.; Lee, S. M.; Yi, C.; Li, C. W. Controllable synthesis of functional nanoparticles by microfluidic platforms for biomedical applications - a review. *Lab Chip* **2017**, *17* (2), 209−226.

(14) Sedelmeier, J.; Ley, S. V.; Baxendale, I. R.; Baumann, M. $KMnO_4$-mediated oxidation as a continuous flow process. *Org. Lett.* **2010**, *12* (16), 3618−3621.

(15) Zhao, C.-X.; He, L.; Qiao, S. Z.; Middelberg, A. P. J. Nanoparticle synthesis in microreactors. *Chem. Eng. Sci.* **2011**, *66* (7), 1463−1479.

(16) Castro, F.; Kuhn, S.; Jensen, K.; Ferreira, A.; Rocha, F.; Vicente, A.; Teixeira, J. A. Process intensification and optimization for hydroxyapatite nanoparticles production. *Chem. Eng. Sci.* **2013**, *100*, 352−359.

(17) Guo, W.; Zhang, Z.; Hacking, J.; Heeres, H. J.; Yue, J. Selective fructose dehydration to 5-hydroxymethylfurfural from a fructose-glucose mixture over a sulfuric acid catalyst in a biphasic system: Experimental study and kinetic modelling. *Chemical Engineering Journal* **2021**, *409*, 128182.

(18) Cherkasov, N.; Denissenko, P.; Deshmukh, S.; Rebrov, E. V. Gas-liquid hydrogenation in continuous flow − The effect of mass transfer and residence time in powder packed-bed and catalyst-coated reactors. *Chemical Engineering Journal* **2020**, *379*, 122292.

(19) Márquez, N.; Castaño, P.; Moulijn, J. A.; Makkee, M.; Kreutzer, M. T. Transient behavior and stability in miniaturized multiphase packed bed reactors. *Industrial & engineering chemistry research* **2010**, *49* (3), 1033−1040.

(20) Yap, S. K.; Yuan, Y.; Zheng, L.; Wong, W. K.; Zhang, J.; Yan, N.; Khan, S. A. Rapid nanoparticle-catalyzed hydrogenations in

triphasic millireactors with facile catalyst recovery. *Green Chem.* **2014**, *16* (11), 4654−4658.

(21) Enache, D. I.; Hutchings, G. J.; Taylor, S. H.; Stitt, E. H. The hydrogenation of isophorone to trimethyl cyclohexanone using the downflow single capillary reactor. *Catal. Today* **2005**, *105* (3−4), 569−573.

(22) Quinson, J.; Neumann, S.; Wannmacher, T.; Kacenauskaite, L.; Inaba, M.; Bucher, J.; Bizzotto, F.; Simonsen, S. B.; Theil Kuhn, L.; Bujak, D.; Zana, A.; Arenz, M.; Kunz, S. Colloids for catalysts: A concept for the preparation of superior catalysts of industrial relevance. *Angew. Chem., Int. Ed. Engl.* **2018**, *57* (38), 12338−12341.

(23) Axet, M. R.; Philippot, K. Catalysis with Colloidal Ruthenium Nanoparticles. *Chem. Rev.* **2020**, *120* (2), 1085−1145.

(24) Ali, A. R. I.; Salam, B. A review on nanofluid: preparation, stability, thermophysical properties, heat transfer characteristics and application. *SN Applied Sciences* **2020**, *2* (10), 1−17.

(25) Pu, X.; Su, Y. Heterogeneous catalysis in microreactors with nanofluids for fine chemicals syntheses: Benzylation of toluene with benzyl chloride over silica-immobilized $FeCl_3$ catalyst. *Chem. Eng. Sci.* **2018**, *184*, 200−208.

(26) Huang, M.; Zhu, C.; Fu, T.; Ma, Y. Enhancement of gas-liquid mass transfer by nanofluids in a microchannel under Taylor flow regime. *Int. J. Heat Mass Transfer* **2021**, *176*, 121435.

(27) Rodriguez, A. M. B.; Binks, B. P. Catalysis in Pickering emulsions. *Soft Matter* **2020**, *16* (45), 10221−10243.

(28) Chang, F.; Vis, C. M.; Ciptonugroho, W.; Bruijnincx, P. C. A. Recent developments in catalysis with Pickering Emulsions. *Green Chem.* **2021**, *23* (7), 2575−2594.

(29) Hiebler, K.; Lichtenegger, G. J.; Maier, M. C.; Park, E. S.; Gonzales-Groom, R.; Binks, B. P.; Gruber-Woelfler, H. Heterogeneous Pd catalysts as emulsifiers in Pickering emulsions for integrated multistep synthesis in flow chemistry. *Beilstein J. Org. Chem.* **2018**, *14*, 648−658.

(30) Vis, C. M.; Nieuwelink, A. E.; Weckhuysen, B. M.; Bruijnincx, P. C. A. Continuous flow Pickering emulsion catalysis in droplet microfluidics studied with In Situ raman microscopy. *Chem. - Eur. J.* **2020**, *26* (66), 15099−15102.

(31) Liedtke, A.-K.; Bornette, F.; Philippe, R.; de Bellefon, C. Gas−liquid−solid "slurry Taylor" flow: Experimental evaluation through the catalytic hydrogenation of 3-methyl-1-pentyn-3-ol. *Chemical Engineering Journal* **2013**, *227*, 174−181.

(32) Ufer, A.; Mendorf, M.; Ghaini, A.; Agar, D. W. Liquid/Liquid slug flow capillary microreactor. *Chem. Eng. Technol.* **2011**, *34* (3), 353−360.

(33) Pieber, B.; Shalom, M.; Antonietti, M.; Seeberger, P. H.; Gilmore, K. Continuous heterogeneous photocatalysis in serial micro-batch reactors. *Angew. Chem., Int. Ed. Engl.* **2018**, *57* (31), 9976−9979.

(34) Li, M.; Zhang, Y.; Zhang, J.; Peng, M.; Yan, L.; Tang, Z.; Wu, Q. Continuous gas−liquid−solid slug flow for sustainable heterogeneously catalyzed PET-RAFT polymerization. *Ind. Eng. Chem. Res.* **2021**, *60* (15), 5451−5462.

(35) Conrad, J. C.; Ferreira, S. R.; Yoshikawa, J.; Shepherd, R. F.; Ahn, B. Y.; Lewis, J. A. Designing colloidal suspensions for directed materials assembly. *Curr. Opin. Colloid Interface Sci.* **2011**, *16* (1), 71−79.

(36) Kakati, H.; Mandal, A.; Laik, S. Promoting effect of Al2O3/ZnO-based nanofluids stabilized by SDS surfactant on $CH_4+C_2H_6+C_3H_8$ hydrate formation. *Journal of Industrial and Engineering Chemistry* **2016**, *35*, 357−368.

(37) Wang, J.; Li, G.; Li, T.; Zeng, M.; Sundén, B. Effect of various surfactants on stability and thermophysical properties of nanofluids. *J. Therm. Anal. Calorim.* **2021**, *143* (6), 4057−4070.

(38) Zong, J.; Yue, J. Gas-liquid slug flow studies in microreactors: Effect of nanoparticle addition on flow pattern and pressure drop. *Frontiers in Chemical Engineering* **2022**, *3*, 788241.

(39) Noroozi, M.; Radiman, S.; Zakaria, A. J. J. o. N. Influence of sonication on the stability and thermal properties of Al_2O_3 nanofluids. *J. Nanomater.* **2014**, *2014*, 1−10.

(40) Asadi, A.; Alarifi, I. M. Effects of ultrasonication time on stability, dynamic viscosity, and pumping power management of MWCNT-water nanofluid: An experimental study. *Sci. Rep.* **2020**, *10* (1), 15182.

(41) Xian, H. W.; Sidik, N. A. C.; Saidur, R. Impact of different surfactants and ultrasonication time on the stability and thermophysical properties of hybrid nanofluids. *Int. Commun. Heat Mass Transfer* **2020**, *110*, 104389.

(42) Mukherjee, S.; Mishra, P. C.; Chakrabarty, S.; Chaudhuri, P. Effects of sonication period on colloidal stability and thermal conductivity of SiO_2−water nanofluid: An experimental investigation. *Journal of Cluster Science* **2021**, 1−9.

(43) Heidarian, A.; Rafee, R.; Valipour, M. S. Hydrodynamic analysis of the nanofluids flow in a microchannel with hydrophobic and superhydrophobic surfaces. *Journal of the Taiwan Institute of Chemical Engineers* **2021**, *124*, 266−275.

(44) Kreutzer, M. T.; Kapteijn, F.; Moulijn, J. A.; Heiszwolf, J. J. Multiphase monolith reactors: Chemical reaction engineering of segmented flow in microchannels. *Chem. Eng. Sci.* **2005**, *60* (22), 5895−5916.

(45) Liu, Y.; Chen, G.; Yue, J. Manipulation of gas-liquid-liquid systems in continuous flow microreactors for efficient reaction processes. *Journal of Flow Chemistry* **2020**, *10* (1), 103−121.

(46) Sadegh Moghanlou, F.; Noorzadeh, S.; Ataei, M.; Vajdi, M.; Shahedi Asl, M.; Esmaeilzadeh, E. Experimental investigation of heat transfer and pressure drop in a minichannel heat sink using Al_2O_3 and TiO_2−water nanofluids. *Journal of the Brazilian Society of Mechanical Sciences and Engineering* **2020**, *42* (6), 1−11.

(47) Kreutzer, M. T.; Kapteijn, F.; Moulijn, J. A.; Kleijn, C. R.; Heiszwolf, J. J. Inertial and interfacial effects on pressure drop of Taylor flow in capillaries. *AIChE J.* **2005**, *51* (9), 2428−2440.

(48) Warnier, M.; De Croon, M.; Rebrov, E.; Schouten, J. Pressure drop of gas−liquid Taylor flow in round micro-capillaries for low to intermediate Reynolds numbers. *Microfluid. Nanofluid.* **2010**, *8* (1), 33−45.

(49) Yap, S. K.; Wong, W. K.; Ng, N. X. Y.; Khan, S. A. Three-phase microfluidic reactor networks − Design, modeling and application to scaled-out nanoparticle-catalyzed hydrogenations with online catalyst recovery and recycle. *Chem. Eng. Sci.* **2017**, *169*, 117−127.

(50) Karan, D.; Khan, S. A. Mesoscale triphasic flow reactors for metal catalyzed gas−liquid reactions. *Reaction Chemistry & Engineering* **2019**, *4* (7), 1331−1340.

(51) Pu, X.; Zhang, B.; Su, Y. Heterogeneous photocatalysis in microreactors for efficient reduction of nitrobenzene to aniline: Mechanisms and energy efficiency. *Chem. Eng. Technol.* **2019**, *42* (10), 2146−2153.

(52) Wood, A. B.; Plummer, S.; Robinson, R. I.; Smith, M.; Chang, J.; Gallou, F.; Lipshutz, B. H. Continuous slurry plug flow Fe/ppm Pd nanoparticle-catalyzed Suzuki−Miyaura couplings in water utilizing novel solid handling equipment. *Green Chem.* **2021**, *23* (19), 7724−7730.

(53) Scheiff, F.; Agar, D. W. Solid particle handling in microreaction technology: Practical challenges and application of microfluid segments for particle-based processes. *Micro-Segmented Flow* **2014**, 103−148.

(54) Zhang, J.; Hassan, M. R.; Rallabandi, B.; Wang, C. Migration of ferrofluid droplets in shear flow under a uniform magnetic field. *Soft Matter* **2019**, *15* (11), 2439−2446.

(55) Boonen, E.; Van Puyvelde, P.; Moldenaers, P. Droplet dynamics in mixed flow conditions: Effect of shear/elongation balance and viscosity ratio. *J. Rheol.* **2010**, *54* (6), 1285−1306.

(56) Hassan, M. R. Magnetic field induced ferrofluid droplet breakup in a simple shear flow at a low Reynolds number. *Phys. Fluids* **2019**, *31* (12), 127104.

(57) Pang, C.; Lee, J. W.; Kang, Y. T. Review on combined heat and mass transfer characteristics in nanofluids. *International Journal of Thermal Sciences* **2015**, *87*, 49−67.

(58) Jiang, J.-Z.; Zhang, S.; Fu, X.-L.; Liu, L.; Sun, B.-M. Review of gas−liquid mass transfer enhancement by nanoparticles from macro to microscopic. *Heat and Mass Transfer* **2019**, *55* (8), 2061−2072.

(59) Cheng, S.-Y.; Liu, Y.-Z.; Qi, G.-S. Progress in the enhancement of gas−liquid mass transfer by porous nanoparticle nanofluids. *J. Mater. Sci.* **2019**, *54* (20), 13029−13044.

(60) Dong, C.; Zhang, J. S.; Wang, K.; Luo, G. S. Micromixing performance of nanoparticle suspensions in a micro-sieve dispersion reactor. *Chemical Engineering Journal* **2014**, *253*, 8−15.

(61) Azimi, N.; Rahimi, M.; Abdollahi, N. Using magnetically excited nanoparticles for liquid−liquid two-phase mass transfer enhancement in a Y-type micromixer. *Chemical Engineering and Processing: Process Intensification* **2015**, *97*, 12−22.

(62) Chong, W. H.; Huang, Y.; Wong, T. N.; Ooi, K. T.; Zhu, G. P. J. A. M. T. Magnetic nanorobots, generating vortexes inside nanoliter droplets for effective mixing. *Adv. Mater. Technol.* **2018**, *3* (4), 1700312.

(63) Hajiani, P.; Larachi, F. Remotely excited magnetic nanoparticles and gas−liquid mass transfer in Taylor flow regime. *Chem. Eng. Sci.* **2013**, *93*, 257−265.

(64) Rahimi, M.; Jafari, O.; Mohammdifar, A. Intensification of liquid-liquid mass transfer in micromixer assisted by ultrasound irradiation and Fe₃O₄ nanoparticles. *Chemical Engineering and Processing: Process Intensification* **2017**, *111*, 79−88.

(65) Reina, A.; Favier, I.; Teuma, E.; Gómez, M.; Conte, A.; Pichon, L. Hydrogenation reactions catalyzed by colloidal palladium nanoparticles under flow regime. *AIChE J.* **2019**, *65* (11), e16752.

(66) Albert, C.; Beladjine, M.; Tsapis, N.; Fattal, E.; Agnely, F.; Huang, N. Pickering emulsions: Preparation processes, key parameters governing their properties and potential for pharmaceutical applications. *J. Controlled Release* **2019**, *309*, 302−332.

(67) Zhang, M.; Ettelaie, R.; Dong, L.; Li, X.; Li, T.; Zhang, X.; Binks, B. P.; Yang, H. Pickering emulsion droplet-based biomimetic microreactors for continuous flow cascade reactions. *Nat. Commun.* **2022**, *13*, 475.

(68) Sun, W.; Zhang, X.; Yao, C.; Wang, Q.; Jin, N.; Lv, H.; Zhao, Y. Hydrodynamic characterization of continuous flow of Pickering droplets with solid nanoparticles in microchannel reactors. *Chem. Eng. Sci.* **2021**, *245*, 116838.

(69) Zhang, M.; Wei, L.; Chen, H.; Du, Z.; Binks, B. P.; Yang, H. Compartmentalized droplets for continuous flow liquid-liquid interface catalysis. *J. Am. Chem. Soc.* **2016**, *138* (32), 10173−10183.

(70) Fapojuwo, D. P.; Oseghale, C. O.; Akinnawo, C. A.; Meijboom, R. Bimetallic PdM (M = Co, Ni) catalyzed hydrogenation of nitrobenzene at the water/oil interface in a Pickering emulsion. *Colloids Surf., A* **2021**, *619*, 126513.

(71) Poulichet, V.; Garbin, V. Ultrafast desorption of colloidal particles from fluid interfaces. *Proc. Natl. Acad. Sci. U. S. A.* **2015**, *112* (19), 5932−5937.

(72) Frelichowska, J.; Bolzinger, M.-A.; Chevalier, Y. Effects of solid particle content on properties of o/w Pickering emulsions. *J. Colloid Interface Sci.* **2010**, *351* (2), 348−356.

(73) Binks, B. P.; Whitby, C. P. Silica particle-stabilized emulsions of silicone oil and water: aspects of emulsification. *Langmuir* **2004**, *20* (4), 1130−1137.

(74) Petzold, M.; Röhl, S.; Hohl, L.; Stehl, D.; Lehmann, M.; von Klitzing, R.; Kraume, M. Mass transfer and drop size distributions in reactive nanoparticle-stabilized multiphase systems. *Chemie Ingenieur Technik* **2017**, *89* (11), 1561−1573.

(75) Zhang, J.; Li, Z.; Cui, X.; Li, J.; Jia, S.; Wang, Y.; Wang, H.; Hou, X.; Deng, T. Mass transfer intensification by microinterface: Efficient dehydration of glycerol into acrolein in a water/oil pickering emulsion system. *Journal of Cleaner Production* **2019**, *236*, 117611.

(76) Peng, Z.; Wang, G.; Moghtaderi, B.; Doroodchi, E. A review of microreactors based on slurry Taylor (segmented) flow. *Chem. Eng. Sci.* **2022**, *247*, 117040.

(77) Kurup, G. K.; Basu, A. S. Field-free particle focusing in microfluidic plugs. *Biomicrofluidics* **2012**, *6* (2), 022008.

(78) Peng, Z.; Moghtaderi, B.; Doroodchi, E. Suspension stability of slurry Taylor flow: A theoretical analysis. *Chem. Eng. Sci.* **2017**, *174*, 459−471.

(79) Can, T.; Mingyan, L.; Yonggui, X. 3-D numerical simulations on flow and mixing behaviors in gas-liquid-solid microchannels. *AIChE J.* **2013**, *59* (6), 1934−1951.

(80) Peng, Z.; Ge, L.; Moreno-Atanasio, R.; Evans, G.; Moghtaderi, B.; Doroodchi, E. VOF-DEM study of solid distribution characteristics in slurry Taylor flow-based multiphase microreactors. *Chemical Engineering Journal* **2020**, *396*, 124738.

(81) Peng, Z.; Gai, S.; Barma, M.; Rahman, M. M.; Moghtaderi, B.; Doroodchi, E. Experimental study of gas-liquid-solid flow characteristics in slurry Taylor flow-based multiphase microreactors. *Chemical Engineering Journal* **2021**, *405*, 126646.

(82) Ufer, A.; Sudhoff, D.; Mescher, A.; Agar, D. W. Suspension catalysis in a liquid−liquid capillary microreactor. *Chemical Engineering Journal* **2011**, *167* (2−3), 468−474.

(83) Olivon, K.; Sarrazin, F. Heterogeneous reaction with solid catalyst in droplet-flow millifluidic device. *Chemical Engineering Journal* **2013**, *227*, 97−102.

(84) Liedtke, A.-K.; Bornette, F.; Philippe, R.; de Bellefon, C. External liquid solid mass transfer for solid particles transported in a milli-channel within a gas−liquid segmented flow. *Chemical Engineering Journal* **2016**, *287*, 92−102.

(85) Liedtke, A.-K.; Scheiff, F.; Bornette, F.; Philippe, R.; Agar, D. W.; de Bellefon, C. Liquid−solid mass transfer for microchannel suspension catalysis in gas−liquid and liquid−liquid segmented flow. *Ind. Eng. Chem. Res.* **2015**, *54* (17), 4699−4708.

(86) Cai, W.; Zhang, J.; Zhang, X.; Wang, Y.; Qi, X. Enhancement of CO₂ Absorption under Taylor Flow in the Presence of Fine Particles. *Chinese Journal of Chemical Engineering* **2013**, *21* (2), 135−143.

(87) Van Pelt, S.; Derks, R.; Matteucci, M.; Hansen, M. F.; Dietzel, A. Flow-orthogonal bead oscillation in a microfluidic chip with a magnetic anisotropic flux-guide array. *Biomed. Microdevices* **2011**, *13* (2), 353−359.

(88) Lisk, P.; Bonnot, E.; Rahman, M. T.; Pollard, R.; Bowman, R.; Degirmenci, V.; Rebrov, E. V. Magnetic actuation of catalytic microparticles for the enhancement of mass transfer rate in a flow reactor. *Chemical Engineering Journal* **2016**, *306*, 352−361.

(89) Buisson, B.; Donegan, S.; Wray, D.; Parracho, A.; Gamble, J.; Caze, P.; Jorda, J.; Guermeur, C. Slurry hydrogenation in a continuous flow reactor for pharmaceutical application. *Chimica Oggi-chemistry Today* **2009**, *27* (6), 12−16.

(90) Calabrese, G. S.; Pissavini, S. From batch to continuous flow processing in chemicals manufacturing. *AIChE J.* **2011**, *57* (4), 828−834.

(91) Salique, F.; Musina, A.; Winter, M.; Yann, N.; Roth, P. M. C. Continuous hydrogenation: Triphasic system optimization at kilo lab scale using a slurry solution. *Frontiers in Chemical Engineering* **2021**, *3*, 1−14.

(92) Enache, D. I.; Hutchings, G. J.; Taylor, S. H.; Natividad, R.; Raymahasay, S.; Winterbottom, J. M.; Stitt, E. H. Experimental evaluation of a three-phase downflow capillary reactor. *Industrial & engineering chemistry research* **2005**, *44* (16), 6295−6303.

(93) Enache, D. I.; Hutchings, G. J.; Taylor, S. H.; Raymahasay, S.; Winterbottom, J. M.; Mantle, M. D.; Sederman, A. J.; Gladden, L. F.; Chatwin, C.; Symonds, K. T.; Stitt, E. H. Multiphase hydrogenation of resorcinol in structured and heat exchange reactor systems. *Catal. Today* **2007**, *128* (1−2), 26−35.

(94) Pollington, S. D.; Enache, D. I.; Landon, P.; Meenakshisundaram, S.; Dimitratos, N.; Wagland, A.; Hutchings, G. J.; Stitt, E. H. Enhanced selective glycerol oxidation in multiphase structured reactors. *Catal. Today* **2009**, *145* (1−2), 169−175.

(95) Chen, Y.; Zhang, Y.; Zou, H.; Li, M.; Wang, G.; Peng, M.; Zhang, J.; Tang, Z. Tuning the gas-liquid-solid segmented flow for enhanced heterogeneous photosynthesis of Azo- compounds. *Chemical Engineering Journal* **2021**, *423*, 130226.

(96) Dong, Z.; Zondag, S. D. A.; Schmid, M.; Wen, Z.; Noël, T. A meso-scale ultrasonic milli-reactor enables gas−liquid-solid photo-

catalytic reactions in flow. *Chemical Engineering Journal* **2022**, *428*, 130968.

(97) Chausse, V.; Llorca, J. Photoproduction of hydrogen in microreactors: Catalytic coating or slurry configuration? *Catal. Today* **2022**, *383*, 156−163.

(98) Nieuwelink, A. E.; Vollenbroek, J. C.; Ferreira de Abreu, A. C.; Tiggelaar, R. M.; van den Berg, A.; Odijk, M.; Weckhuysen, B. M. Single catalyst particle diagnostics in a microreactor for performing multiphase hydrogenation reactions. *Faraday Discuss.* **2021**, *229*, 267−280.

(99) Senthilraja, S.; Vijayakumar, K.; Gangadevi, R. A comparative study on thermal conductivity of Al₂O₃/water, CuO/water and Al₂O₃−CuO/water nanofluids. *Digest Journal of Nanomaterials and Biostructures* **2015**, *10* (4), 1449−1458.

(100) Banakar, V.; Sabnis, S.; Gogate, P.; Raha, A. Ultrasound assisted continuous processing in microreactors with focus on crystallization and chemical synthesis: A critical review. *Chem. Eng. Res. Des.* **2022**, *182*, 273.

(101) Rossi, D.; Jamshidi, R.; Saffari, N.; Kuhn, S.; Gavriilidis, A.; Mazzei, L. Continuous-flow sonocrystallization in droplet-based microfluidics. *Cryst. Growth Des.* **2015**, *15* (11), 5519−5529.

(102) Cains, P. W.; Martin, P. D.; Price, C. J. The use of ultrasound in industrial chemical synthesis and crystallization. 1. Applications to synthetic chemistry. *Organic process research & development* **1998**, *2* (1), 34−48.

(103) Dong, Z.; Udepurkar, A. P.; Kuhn, S. Synergistic effects of the alternating application of low and high frequency ultrasound for particle synthesis in microreactors. *Ultrasonics Sonochemistry* **2020**, *60*, 104800.

(104) Dong, Z.; Rivas, D. F.; Kuhn, S. Acoustophoretic focusing effects on particle synthesis and clogging in microreactors. *Lab Chip* **2019**, *19* (2), 316−327.

(105) Ariyaratne, C.; Jones, T. J. A. j. Design and optimization of swirl pipe geometry for particle-laden liquids. *AIChE J.* **2007**, *53* (4), 757−768.

(106) Yan, F.; Su, S.; Tang, W.; Zhu, R.; Chen, Q.; Yin, J.; Wang, L. Enhancement of liquid-solid two-phase flow through a vertical swirling pipe. *Journal of Applied Fluid Mechanics* **2020**, *13* (5), 1501−1513.

(107) Shi, H.; Yuan, J.; Li, Y. The impact of swirls on slurry flows in horizontal pipelines. *Journal of Marine Science and Engineering* **2021**, *9* (11), 1201.

(108) Hutter, C.; Zenklusen, A.; Kuhn, S.; Rudolf von Rohr, P. Large eddy simulation of flow through a streamwise-periodic structure. *Chem. Eng. Sci.* **2011**, *66* (3), 519−529.

(109) Potdar, A.; Protasova, L. N.; Thomassen, L.; Kuhn, S. Designed porous milli-scale reactors with enhanced interfacial mass transfer in two-phase flows. *Reaction Chemistry & Engineering* **2017**, *2* (2), 137−148.

(110) Clarke, D. A.; Dolamore, F.; Fee, C. J.; Galvosas, P.; Holland, D. J. Investigation of flow through triply periodic minimal surface-structured porous media using MRI and CFD. *Chem. Eng. Sci.* **2021**, *231*, 116264.

(111) de Abreu, W. C.; Garcia, M. A.; Nicolodi, S.; de Moura, C. V.; de Moura, E. M. J. R. a. Magnesium surface enrichment of CoFe₂O₄ magnetic nanoparticles immobilized with gold: Reusable catalysts for green oxidation of benzyl alcohol. *RSC Adv.* **2018**, *8* (7), 3903−3909.

(112) Liu, Y.; Lv, M.; Li, L.; Yu, H.; Wu, Q.; Pang, J.; Liu, Y.; Xie, C.; Yu, S.; Liu, S. Synthesis of a highly active amino-functionalized Fe₃O₄@SiO₂/APTS/Ru magnetic nanocomposite catalyst for hydrogenation reactions. *Appl. Organomet. Chem.* **2019**, *33* (4), e4686.

(113) Gonzalez Ortiz, D.; Pochat-Bohatier, C.; Cambedouzou, J.; Bechelany, M.; Miele, P. Current trends in Pickering emulsions: Particle morphology and applications. *Engineering* **2020**, *6* (4), 468−482.

(114) Dong, Z.; Wen, Z.; Zhao, F.; Kuhn, S.; Noël, T. Scale-up of micro- and milli-reactors: An overview of strategies, design principles and applications. *Chemical Engineering Science: X* **2021**, *10*, 100097.

(115) Markowz, G.; Schirrmeister, S.; Albrecht, J.; Becker, F.; Schütte, R.; Caspary, K. J.; Klemm, E. Microstructured reactors for heterogeneously catalyzed gas-phase reactions on an industrial scale. *Chemical Engineering & Technology: Industrial Chemistry-Plant Equipment-Process Engineering-Biotechnology* **2005**, *28* (4), 459−464.

(116) Woitalka, A.; Kuhn, S.; Jensen, K. F. Scalability of mass transfer in liquid−liquid flow. *Chem. Eng. Sci.* **2014**, *116*, 1−8.

(117) Jorda, J.; Vizza, A. From laboratory to production: a seamless scale-up. *Speciality Chemicals Magazine* **2012**, 19−21.

(118) Steiner, A.; Roth, P. M.; Strauss, F. J.; Gauron, G.; Tekautz, G. n.; Winter, M.; Williams, J. D.; Kappe, C. O. Multikilogram per hour continuous photochemical benzylic brominations applying a smart dimensioning scale-up strategy. *Org. Process Res. Dev.* **2020**, *24* (10), 2208−2216.